HERRINGTON EDITED

Fluorescence *in situ* Hybridization in Surgical Pathology: Principles and Applications

Liang Cheng, [1,2], Shaobo Zhang, [1], Lisha Wang, [3], Gregory T MacLennan, [4], Darrell D. Davidson, [1]

[1]Department of Pathology and Laboratory Medicine, [2]Department of Urology, Indiana University School of Medicine, Indianapolis, Indiana; [3]Michigan Center for Translational Pathology, University of Michigan, Ann Arbor, MI; [4]Departments of Pathology and Laboratory Medicine, Case Western Reserve University, Cleveland, Ohio.

Running Head: FISH in Surgical Pathology

Total number of text pages, 46; Number of tables, 2; Number of figures, 6.

Address correspondence and reprint requests to Liang Cheng, M.D., Department of Pathology and Laboratory Medicine, Indiana University School of Medicine, 350 West 11th Street, IUHPL Room 4010, Indianapolis, IN 46202, USA. Telephone: 317-491-6442; Fax: 317-491-6419; E-mail: liang_cheng@yahoo.com

ABSTRACT

Identification of recurrent tumour-specific chromosomal translocations and novel fusion oncogenes has important diagnostic, therapeutic, and prognostic implications. Over the past decade, fluorescence *in situ* hybridization (FISH) analysis of tumour samples has been one of the most rapidly growing areas in genomic medicine and surgical pathology practice. Unlike traditional cytogenetics, FISH affords a rapid analysis of formalin-fixed, paraffin-embedded cells within a routine pathology practice workflow. As more diagnostic and treatment decisions are based on results of FISH, demand for the technology will become more widespread. Common FISH-detected alterations are chromosome deletions, gains, translocations, amplifications, and polysomy. These chromosome alterations may have diagnostic and therapeutic implications for many tumour types. Integrating genomic testing into cancer treatment decisions poses many technical challenges, but rapid progress is being made to overcome these challenges in precision medicine. FISH assessment of chromosomal changes relevant to differential diagnosis and cancer treatment decisions has become an important tool for the surgical pathologist. The aim of this review is to provide a theoretical and practical survey of FISH detected translocations with a focus on strategies for clinical application in surgical pathology practice.

Key Words: Fluorescence in situ hybridization (FISH), molecular genetics/cytogenetics, targeted therapy, precision medicine, differential diagnosis

1. Introduction

In the late 1960s, in situ hybridization was first performed with radioisotope-labeled probes followed by autoradiography.[1-3] Fluorescence-labeled probe technology started in the early 1980s with RNA probes that were directly labeled with fluorophores complementary to specific DNA sequences. Advances in fluorescence microscopy and digital imaging, as well as widespread availability of genomic and bioinformatic resources, have greatly improved the resolution, sensitivity, specificity, and accessibility of fluorescence *in situ* hybridization (FISH).

Interphase FISH, hereinafter simply referred to as FISH, is the usual clinical application of this diagnostic tool.[4] FISH involves the use of fluorescence labeled fragments of DNA (probes) binding to interphase chromosomes of cytology specimens or paraffin embedded tissue sections. Common FISH-detected alterations are chromosome deletions, gains, translocations, amplifications, and polysomy. These chromosome alterations may have diagnostic and therapeutic implications for many tumour types[5, 6]. Integrating precise genomic testing into cancer treatment decisions poses many technical challenges, but rapid progress is being made in overcoming these difficulties. This review focuses on FISH based detection of translocations applicable to surgical pathology.

2. Chromosomal translocations: An overview

Chromosomal translocation refers to a chromosome rearrangement involving nonhomologous chromosome parts. Translocations can be balanced, without net loss of material, or unbalanced, with gain or loss of genetic loci. Translocation often creates fusion genes when two otherwise separated chromosome parts join.[7-9] These fusion genes may behave as a hybrid chimeric

oncogene, inducing tumorigenesis by gene overexpression, or they may interrupt an important control region, causing unresponsiveness to regulatory control factors. For example, receptor tyrosine kinase gain of function fusion oncogenes are a mechanism whereby mesenchymal cells may be transformed into sarcomas. Constitutive activation of the insulin family kinase *ALK* results from unregulated dimerization of the fusion gene protein containing the active ALK kinase domain. This mechanism underlies about half of inflammatory myofibroblastic tumours. Most Ewing sarcoma cases result from *EWSR1-FLI1* gene fusion deregulating the ETS transcription factor *FLI1*, leading to aberrant expression of Ewing sarcoma transforming genes. The pathognomonic fusion protein of dermatofibrosarcoma protuberans (DFSP) is *PDGFB-COL1A1*. This amalgamation of the essential fibroblast collagen gene (*COL1A1*) with the angiogenic growth factor gene (*PDGFB*) leads to increased growth factor release. An overabundance of growth factor results in overstimulation of receptor tyrosine kinase PDGFR, activating not only endothelial cells but also fibroblasts and inflammatory cells.[10]

Translocations may involve two different chromosomes or may exchange information between regions in the same chromosome. Intrachromosomal rearrangement may cause transposition of the involved loci with or without centromere involvement. Chromosome rearrangement, whether intrachromosomal or between chromosomes, invariably leads to a neoteric juxtaposition of previously unrelated gene elements into a new fusion gene that may or may not be transcribed. Fusion gene detection, therefore, is at the heart of FISH diagnostic testing.

Chromosomal translocation is detectable by several methods, including FISH, metaphase karyotyping, microarray comparative genomic hybridization, SNP-array, and next generation sequencing[10-20]. Some chromosomal translocations are not detectable by FISH, whether by split-

apart (Some chromosomal translocations are not detectable by FISH, whether by split-apart (**Fig. 1**) or by fusion probes (**Fig. 2**). To be a reliable diagnostic tool, the probe sets must reproducibly show either an increase or a decrease in the optical distance between probe signals. Some translocations, especially those involving intrachromosomal inversion or deletion, have a relatively short physical distance between the fusion partners after translocation. These small distances cannot reliably be resolved at the light microscopic level. In this scenario, a PCR-based method is favoured. RNA-seq, a next generation sequencing technique, can detect both known and novel gene fusion events and allows RNA analysis through cDNA sequencing at a comprehensive genome-wide scale. It can detect both cryptic intrachromosomal rearrangements and some fusion products with uncharacterized fusion partners[14, 21-26]. (**Fig. 1**) or by fusion probes (**Fig. 2**). To be a reliable diagnostic tool, the probe sets must reproducibly show either increased or decreased the optical distance between probe signals. Some translocations, especially those involving intrachromosomal inversion or deletion, have a relatively short physical distance between the fusion partners after translocation. These small distances cannot reliably be resolved at the light microscopic level. In this scenario, a PCR-based method is favored. RNA-seq, a next generation sequencing technique, can detect both known and novel gene fusion events and allow RNA analysis through cDNA sequencing at a comprehensive genome-wide scale. It can detect both cryptic intrachromosomal rearrangements and some fusion products with uncharacterized fusion partners.

3. Chromosomal translocations mainly associated with sarcomas

About 30% of sarcomas have well documented specific translocations, and the percentage continues to grow. With some exceptions, sarcoma translocations form fusion genes with the 5′

gene segment contributing a strong promoter and overexpression of the 3′ proto-oncogene segment by transactivation. Recurrent gene fusions in soft tissue sarcomas tend to occur in tumours sharing similar morphological characteristics.[27] Roughly half of the sarcoma-associated fusion genes contain a member of the *TET* gene family, including *FUS, EWSR1*, and *TAF15* as the proto-oncogene partner. Most fusion genes are strongly associated with a particular tumour type, potentially making them ideal molecular diagnostic markers.[10, 27-29] Some fusion proteins are actual or potential therapeutic targets, making the detection of fusion gene products valuable both for diagnostic and for therapeutic purposes.

More than 400 recurring translocations have been found in soft tissue sarcomas. The challenge now is to identify which of these recurring translocations truly has diagnostic, mechanistic, or therapeutic meaning for the associated sarcomas. Over 30 subtypes of the mesenchymal tumor can be confirmed by FISH analysis based on tumor-specific chimeric fusion sequences.[28] FISH-identifiable sarcomas include many common entities: Ewing sarcoma/primitive neuroectodermal tumor, synovial sarcoma, liposarcoma, round cell Ewing-like sarcoma, pulmonary myxoid sarcoma, inflammatory myofibroblastic tumor, and others (**Table 1**).

3.1 Ewing sarcoma

Ewing sarcomas are composed of small round blue cells with highly malignant behaviour, usually affecting bone and extraosseous tissues of children and young adults. There is a specific balanced chromosomal rearrangement in most Ewing sarcomas, providing a valuable tool for diagnosis. The fusion partners of *EWSR1* belong to several gene families, mainly encoding transcription factors. These proteins join the amino terminal of the *EWSR1* gene with the carboxy terminal of an *ETS* gene family member. This fusion not only abrogates the RNA splicing

function of *EWSS1* but also removes essential trans-activating control regions of the *ETS* gene partner. As many as 90% of the translocations involve the *EWSR1* gene in the form of t(11;22)(q24;q12) translocation, which juxtaposes *EWSR1* at 22q12 with the *FLI1* gene on chromosome 11q24.[30]

The fusion gene encodes a protein containing the upstream amino-terminal domain of *EWSR1* and the downstream carboxy-terminal region of *FLI1*. This fusion protein uniquely functions in controlling cell growth and regulating the transcription of downstream genes responsible for uncontrolled cell division, and survival in the face of otherwise lethal additional mutations. The *ERG* translocation, t(21;22)(q22;12), resulting in *EWSR1-ERG* fusion, represents only 10% of all Ewing sarcomas. The functional consequences of these variant fusion proteins are similar to those of the more common *EWSR1-FLI1* fusion. One study suggested a better outcome for patients with localized tumours expressing the most common t(11;22) transcript (*EWSR1* exon 7 fused to *FLI1* exon 6), but limited prognostic data is currently available for the less common fusion types at this time.[31]

3.2 Myxoid liposarcoma

The diagnosis of myxoid liposarcoma may be challenging by histology alone, especially on small biopsy tissues, since a variety of soft tissue tumours with myxoid change may mimic myxoid liposarcoma. Myxoid liposarcoma represents about 10% of all adult sarcomas and approximately 33% of all liposarcomas. Chromosomal translocations t(12,16)(q13;p11) and t(12;22)(q13;q12), rendering gene fusions of DNA-damage inducible transcript 3 (*DDIT3*) with *FUS* or *EWSR1*, respectively, are characteristic of myxoid liposarcoma; one of these is identifiable in more than

95% of cases. Commonly used FISH probes are included in the Vysis *DDIT3* dual colour, break-apart rearrangement probe kit, t(12;16)(q13;p11).

3.3 Synovial sarcoma

Synovial sarcoma is characterized by t(X;18)(p11;q11) translocation, which is present in virtually all tumours. The translocation fuses synovial sarcoma translocation gene (*SS18*) on chromosome 18 with either synovial sarcoma X breakpoint 1 (*SSX1*) (66%) or *SSX2* (33%), located on chromosome Xp11.[32, 33] The FISH test is highly specific and sensitive for synovial sarcoma. A characteristic t(X;18)(p11;q11) translocation or variants were found in 90% of synovial sarcomas. The t(X;18) translocation has not been found in other sarcomas.

3.4 Solitary fibrous tumour

Solitary fibrous tumour comprises a family of soft tissue lesions usually affecting adults, occurring at any site, and presumed to be of fibroblastic differentiation. The tumours were thought to derive from pericytes, but now there is evidence to support a fibroblastic or myofibroblastic origin. Recurrent fusions of the two genes, NGFI-A–binding protein 2 (*NAB2*) and signal transducer and activator of transcription 6 (*STAT6*), both located near chromosomal region 12q13, have been identified in solitary fibrous tumours. The *NAB2-STAT6* fusion gene is derived from an inverted intrachromosomal fusion of the *NAB2* and *STAT6* genes on 12q13.[34, 35] The fusion product contains the activation domain of *STAT6* fused to the early growth response (EGR)-binding domain of *NAB2[36]*. Overexpression of the *NAB2-STAT6* fusion gene induces cell proliferation and activates expression of *EGFR*-responsive genes. Chmielecki et al identified the *NAB2-STAT6* translocation by whole exome sequencing of 17 solitary fibrous

tumours and matched blood.[34] This fusion gene was confirmed in 29 of 55 (55%) solitary

fibrous tumours by exome sequencing. Since the *NAB2* and *STAT6* genes are both located near

12q13, the break apart designed probe may detect some but not all of the *NAB2-STAT6*

translocations. Mohajeri et al used 6 independent molecular genetic techniques directed at *NAB2*

or *STAT6* rearrangement to identify *NAB2–STAT6* fusion in 37 of 41 (90%) of the solitary

fibrous tumours evaluated.[37]

It should be noted that the *NAB2-STAT6* fusion is not consistently detected by FISH due to the

very close proximity of the 2 genes (overlapping ends)[36] and, in this setting, RT-PCR is the

preferred method of detection. STAT6 immunostaining is highly sensitive and specific for

detecting *NAB2-STAT6* fusion product and is now becoming standard practice.

3.5 Round cell Ewing-like sarcoma

There is a small subset of sarcomas that clinically and histologically mimic Ewing sarcoma but

fail to exhibit any of the cytogenetic abnormalities reported for these tumours. Recently cases of

"Ewing-like sarcoma" have been found to have a recurrent chromosomal translocation,

t(4;19)(q35;q13), resulting in fusion of capicua homolog (*CIC*) and double homeobox 4

(*DUX4*).[38] Fusion of the C-terminal fragment of *DUX4* with *CIC* enhances the transcriptional

activity of *CIC* and deregulates expression of its downstream targets. *CIC-DUX4* fusion protein

directly binds the ETS variant 5 (*ETV5*) promoter at a previously unrecognized site and

upregulates expression of this oncogene. Four cases of *CIC-DUX4* sarcoma were identified using

a combination of conventional cytogenetic, reverse transcription polymerase chain reaction (RT-

PCR), and FISH methods.[39] FISH was positive for *CIC-DUX4* fusion in all four tumours. The

distinctive histopathological features and rapid disease progression may warrant classification of *CIC-DUX4* sarcoma as a new translocation-associated sarcoma.

3.6 Inflammatory myofibroblastic tumour

Inflammatory myofibroblastic tumour is a spindle cell neoplasm most frequently found in the urinary bladder but occasionally diagnosed at various body sites. Although these tumours usually behave in a benign fashion, they may be difficult to differentiate from sarcoma or sarcomatoid carcinoma. Roughly half of inflammatory myofibroblastic tumours have *ALK* rearrangements leading to elevated expression of ALK chimeric protein.[40] The *ALK* translocations involve 2p23 with multiple fusion partners, including *TPM3-ALK, RANBP2-ALK, TPM4-ALK, EML4-ALK, CLTC-ALK, CARS-ALK, ATIC-ALK, SEC31A-ALK,* and *PPFIBP1-ALK.[41, 42]* In each instance, the fusion gene overexpresses *ALK* due to promoter swapping. *ALK* rearrangements may prove useful for distinguishing inflammatory myofibroblastic tumour from morphologically similar neoplasms.

Therapy targeting tumour cells with *ALK* gene rearrangement has been shown to induce partial tumour remission.[43, 44] Currently, little is known about the pathogenesis of the 50% of inflammatory myofibroblastic tumours that lack *ALK* translocation.

Besides *ALK*, *ROS1* and *NTRK3* gene rearrangements, *YWHAE–ROS1* and *ETV6–NTRK3* are also found in ALK fusion negative inflammatory myofibroblastic tumours.[45] Antonescu et al reported six (10%) *ROS1* related translocations in a group of 62 cases. Most of the patients were

children, and the tumours were located in the lung or abdomen.[46] Two (3.2%) inflammatory myofibroblastic tumour cases showed *TFG-ROS1* fusions, t(3;6)(q12;q22).

3.7 Alveolar soft part sarcoma

Alveolar soft part sarcoma has a characteristic histopathology but a controversial histogenesis. Alveolar soft part sarcomas arising in many body sites have a diagnostic translocation. The rearrangement involves the alveolar soft part sarcoma locus (*ASPSCR1*) located on chromosome 17q25 and the transcription factor for the immunoglobulin heavy chain enhancer 3 (*TFE3*) gene, located on chromosome Xp11.[47] The fusion protein is capable of inducing aberrant transcription of *TFE3*-regulated genes and may confer resistance to cell-cycle arrest signals and override arrest. Selvarajah et al investigated 17 alveolar soft part sarcomas from 11 patients by array comparative genomic hybridization and FISH. FISH identified the *ASPSCR1-TFE3* fusion in all cases.[12]

The *TFE3-ASPSCR1* [der(17)t(X;17)(p11;q25)] translocation is found in 80% of alveolar soft part sarcomas. This translocation is also found in a distinctive subset of renal cell carcinoma (translocation renal cell carcinoma) which frequently has a papillary architecture.

3.8 Alveolar Rhabdomyosarcoma

Alveolar rhabdomyosarcoma (ARMS) is a highly aggressive soft tissue sarcoma associated with translocations involving *PAX3-FOXO1* [t(2;13)(q35;q14)] or *PAX7-FOXO1* [t(1;13)(p36;q14)] reportedly accounting for 55-80% and 15-22% of ARMS, respectively.[48] These translocations generate fusion proteins that function as transcriptional activators with oncogenic effects. FISH

testing has higher sensitivity and specificity than RT-PCR assay for these fusion transcripts.[49]

FISH analysis using the *FOXO1* split-apart probe adds the ability to detect variant *FOXO1*

rearrangements not detectable by PCR.

3.9 Clear cell sarcoma of soft tissue

Clear cell sarcoma of soft tissue is a rare mesenchymal malignancy mainly occurring in young to

middle-aged adults of either sex, typically in the soft tissue of the lower extremities. The tumour

is aggressive with a high frequency of local recurrence and distant metastasis. Almost all (90%)

clear cell sarcomas are associated with *EWSR1-ATF1* translocation, t(12;22)(q13;q12), while a

smaller subset of tumours (6%) bear an *EWSR1-CREB1* translocation.[50] The specific

translocation is unrelated to tumour prognosis. In a group of 33 clear cell sarcomas, RT-PCR

using RNA extracted from formalin-fixed, paraffin-embedded tissues demonstrated transcripts of

the *EWSR1-ATF1* (31/33) or *EWSR1-CREB1* fusion gene (2/33).[51]

4. Chromosomal translocations in other solid tumours

A growing number of fusion oncogenes have been also associated with some common adult

epithelial cancers, such as adenocarcinomas of the lung, prostate, colon, kidney, breast, and other

epithelial solid tumours (**Table 2**).

4.1 Chromosomal translocations mainly associated with lung cancer

4.1.1 *EML4-ALK* translocation

Anaplastic lymphoma kinase (ALK) is a tyrosine kinase member of the insulin receptor

superfamily normally expressed only in certain neurons of the developing central nervous

system. Fusions of *ALK* with echinoderm microtubule-associated protein-like 4 (*EML4*), a protein involved in microtubule assembly, results in constitutive activation of the ALK kinase.[52, 53] The *ALK* fusion oncogene was first identified in anaplastic large-cell lymphoma, in which a t(2;5) chromosome rearrangement activates the ALK kinase by fusion with the nucleophosmin gene (*NPM1*) on chromosome 5. *ALK* fusions have been reported in non-small cell lung carcinoma, breast cancer, colorectal cancer, renal cancer, and other tumour types [41, 42, 54, 55]. The common FISH test for *ALK* rearrangement uses dual colour labeled probes covering the *ALK* gene and 3′ flanking region of *ALK* (**Fig. 3**). The year 2013 was the first time that the FDA simultaneously approved a novel anticancer drug (crizotinib, Pfizer) and its companion FISH detection kit (*ALK* FISH probe kit, Abbott Molecular), highlighting the critical role of FISH triage for guiding *ALK*-targeted therapy.[56, 57] A FDA approved Vysis *ALK* break apart FISH probe kit is recommended by the College of American Pathologists (CAP). In general, a sample is considered positive if >15% of cells are positive for *ALK* separation of the green and orange signals.

4.1.2   *ROS1* translocation

C-ROS oncogene 1 (*ROS1*) is a receptor tyrosine kinase of the insulin receptor family. The *ROS1* rearrangements lead to a constitutively activated fusion kinase, and are detected in 1.2–1.7% of lung adenocarcinoma cases.[58-60] *ROS1* activation stimulates other downstream signaling proteins including AKT1, MAPK1, MAPK3, IRS1, and PLCG2.[59] Patients with *ROS1* translocation are significantly younger than most patients with lung cancer and are more likely to be never-smokers. Their cancers tend to be adenocarcinoma, and their tumours have a tendency towards higher grade. Several genes may serve as fusion partners for *ROS1* including *SDC4*,

SLC34A2, *CD74*, *GOPC*, and *EZR*, yet each of the *ROS1* fusion products leads to constitutive ROS kinase activation.[61]   A dual probe break-apart method is used to detect *ROS1* rearrangement as with *ALK* rearrangement. Criteria similar to those used for *ALK* rearrangement screening are used to evaluate the *ROS1* FISH test.

ROS1 fusions are also found in meningioma, cholangiocarcinoma, and glioblastoma, but no systematic investigation of tyrosine kinase inhibitors has been published for *ROS1*-fusion positive tumours of these primary sites.[62, 63] The reported incidence of *ROS1* translocation is also low in other tumour types: 8.7% (2/23) of cholangiocarcinomas, 0.5% (1/200) of ovarian carcinomas, 0.6% (3/495) of gastric adenocarcinomas, 0.8% (2/236) of colorectal carcinomas, 7.7% (2/26) of inflammatory myofibroblastic tumours, 2.9% (1/34) of angiosarcomas, and 5% (1/20) of epithelioid haemangioendotheliomas.[63-66]

4.1.3 *RET* translocation

Novel chromosomal translocations involving the *RET* tyrosine kinase gene were reported recently[61, 67]. The rearranged during transfection (*RET*) gene belongs to the cadherin superfamily, and encodes a cell surface receptor tyrosine kinase that transduces signals for cell growth and differentiation[67, 68]. Several *RET* rearrangements have been identified in non-small cell lung carcinomas, including *KIF5B-RET*, *CCDC6-RET*, *NCOA4-RET*, and *TRIM33-RET*.

RET gene translocation occurs in approximately 1–2% of non-small cell lung carcinomas and defines a clinically distinct subset of non-small cell lung carcinomas. Patients with

adenocarcinomas with *RET* fusion tend to be younger than most patients with lung cancer and they are more likely to be never-smokers.[69] In a study of 936 patients with non-small cell lung carcinoma, the *RET* fusion gene was exclusively detected in 13 patients (11/633, 1.7% in adenocarcinoma; 2/24, 8.3% in adenosquamous cell carcinoma).[70] Of the 13 *RET* fusion-positive patients, 9 (69%) had *KIF5B-RET*, 3 (23%) had *CCDC6-RET*, and 1 (7.6%) had *NCOA4-RET* fusion. Their tumours tended to be poorly differentiated carcinomas that exhibited early lymph node metastasis. Drilon et al found *RET* fusions in 5 of 31 patients and showed that the *RET* kinase can be effectively inhibited by several small molecule inhibitors.[71] Followup imaging conducted after 4 and 12 weeks of therapy confirmed a partial response with a 66% decrease in measurable disease in the lungs and pleura.

4.1.4   *EWSR1-CREB1* translocation in primary pulmonary myxoid sarcomas

In the 2015 World Health Organization (WHO) Classification of Tumours of the Lung, Pleura, Thymus and Heart, pulmonary myxoid sarcoma with *EWSR1-CREB1* translocation was introduced as a new entity.[72] Primary pulmonary myxoid sarcoma is rare, and arises most frequently in young females. The tumour consists of lobules with delicate, lacelike strands and cords of mildly atypical round or spindle cells in a prominent myxoid stroma. In addition to displaying a distinct morphology, it bears a *EWSR1-CREB1* translocation in 70% of cases.[73] It should be noted that *EWSR1-CREB1* translocation is not unique for this entity; it can also be observed in clear cell sarcoma-like tumour of the gastrointestinal tract and angiomatoid fibrous histiocytoma (**Table 1**)

5. Chromosomal translocations mainly associated with kidney cancer

5.1 *TFE3* translocation

Renal cell carcinomas associated with Xp11.2 translocation are uncommon renal tumours that were recognized as a distinct entity in the 2016 World Health Organization classification of Tumours of the Urinary System and Male Genital Organs.[74] These neoplasms comprise the majority of paediatric renal cell carcinomas and a smaller percentage of adult renal cell carcinomas. There are several different translocations involving chromosome Xp11.2, resulting in gene fusions of the *TFE3* gene with various activating partners. At least five different fusion partners for *TFE3* have been characterized, including *ASPSCR1, PRCC, SFPQ, CLTC*, and *NONO* (**Fig. 4**).[75, 76] Variant translocations with unknown fusion partners include t(X;3)(p11.2;q23) and t(X;10)(11.2;q23). Different gene fusions in Xp11.2 translocation renal cell carcinoma may be associated with different morphological features.[77, 78]

The *TFE3* break-apart FISH assay has proven useful for detecting *TFE3* gene fusions in Xp11.2 translocation renal cell carcinoma, and the FISH assay, in comparison with immunohistochemical evaluation, is less often adversely affected by technical and fixation issues. Rao et al analyzed 24 poorly differentiated renal cancers with break-apart *TFE3* FISH.[79] Seventeen cases showed *TFE3* rearrangement associated with Xp11.2 translocation by FISH, including seven previously unclassified renal cell tumours, supporting the diagnostic value and clinical application of FISH for enigmatic renal tumours. On the basis of commercially available and widely tested break-apart FISH assays, the *TFE3* split-signal pattern was considered positive when ≥10% of the tumour nuclei showed separation of the two coloured signals by more than one signal diameter (**Fig. 5**).

5.2 *TFEB* translocation

The t(6;11) translocation renal cell carcinoma is rare and usually bears a translocation between *TFEB* and *MALAT1* on chromosome 11q12, but rarely *TFEB* may partner with *KHDRBS2* on chromosome 6q11 (**Fig. 4B**).[80] Renal cell carcinomas with t(6;11)(p21;q12) are characterized by translocation involving the transcription factor EB (*TFEB*). Identification of either TFEB protein overexpression or t(6;11) translocation is useful for the diagnosis of *TFEB* renal cell carcinoma. Cytogenetic karyotypic analysis and RT-PCR are also common methodologies for identifying this translocation. Unfortunately, these methods are limited by the need for fresh viable tumour cells for culture or flash frozen tissue to quantitatively assay *TFEB* mRNA. More recently, a break-apart FISH assay to detect *TFEB* gene translocation has been validated on formalin-fixed paraffin-embedded tissues, and appears to be superior to the TFEB IHC assay. Rao et al reported seven patients with *TFEB* renal cell carcinoma confirmed diagnostically by using FISH technology. All seven cases were *TFEB* positive by both fusion and split-apart probe designs.[81]

5.3 *SMARCB1/SMARCB1* genetic alterations and ALK translocation

Renal medullary carcinoma is a rare, aggressive tumour with a poor clinical outcome. It belongs to a *SMARCB1*-deficient tumour family.[82] Inactivation of tumour suppressor gene *SMARCB1* is the hallmark of this tumour. Cheng et al studied a total of 19 renal cancers that included 5 renal medullary carcinomas, 2 paediatric rhabdoid tumours of kidney, 10 high grade renal cell carcinomas, and 2 urothelial carcinomas.[83] All renal medullary carcinomas were from African American patients with sickle-cell trait who presented with extensive extrarenal metastases at the time of diagnosis. All five renal medullary carcinomas and two renal rhabdoid tumours showed

complete loss of SMARCB1 expression. Another study by Calderaro et al found recurrent

alterations involving chromosome 22q11 in each of four renal medullary carcinomas associated

with sickle-cell trait. Each of these showed hemizygous *SMARCB1* deletion[84]. RNA

sequencing further identified fusion transcripts involving *SMARCB1* in these tumours. The

transcripts resulted from balanced translocations disrupting *SMARCB1* and fusing it to various

partners including *CAPN2*, *RORA*, *MAML2*, and *MALAT1*.

ALK translocation was also reported in renal medullary carcinomas from young patients with

sickle-cell trait to be associated with *VCL-ALK* translocation.[85] The incidence of *ALK*

rearrangement associated with all renal cell carcinomas is low, with an overall frequency of

<1%. In a study including 534 adult renal cell carcinoma patients, *ALK* rearrangements occurred

in two papillary renal cell carcinomas.[86] More recently, Kusano et al reported 2 cases of RCC

harbouring a novel STRN-ALK fusion.[87] In both cases, the patients were in their 30s at the

time of nephrectomy.

6.   Chromosomal translocations mainly associated with prostate cancer

A significant event in prostate carcinogenesis involves gene fusion between members of the E-

twenty-six transforming factor (*ETS*) family of genes, including *ERG*, and the transmembrane

protease, serine 2 (*TMPRSS2*, 21q22.3) gene[88-91]. The genes involved are the androgen-

regulated gene *TMPRSS2* and *ETS* transcription factor family members, including *ERG*

(21q22.2), *ETV1* (7p21.2), or *ETV4* (17q21). *TMPRSS2-ERG* gene fusion has been identified in

about 50% of prostate tumours (ranging from 27% to 79%). These fusions appear to represent a

specific early event in prostatic carcinogenesis that can be observed in high grade prostatic

intraepithelial neoplasia.[90] The *TMPRSS2*-ERG rearrangement can be identified by both dual

colour split apart probe or by tricolour probes (**Fig. 6**).[92-94]

7. Chromosomal translocations mainly associated with breast cancer

A rare variant of breast cancer, secretory breast cancer, has a characteristic recurrent

translocation between ETS variant 6 (*ETV6*) and neurotrophic tyrosine kinase type 3 (*NTRK3*),

t(12;15)(p13;q25).[95, 96] This translocation appears to be the initial hit required for formation

of secretory breast cancer. Retroviral transfer of *ETV6-NTRK3* into murine mammary epithelial

cells resulted in transformed cells that readily formed tumours in nude mice.

The biological consequence of this translocation is expression of a chimeric tyrosine kinase

protein with potent transforming capability. The fusion protein strongly activates the *MAPK1*

and the *PIK3CA/AKT1* pathways.[96] The occurrence of the *ETV6-NTRK3* translocation and

consequential expression of the oncogene is an initiating event in the genesis of secretory breast

cancer.[97] The *ETV6-NTRK3* translocation is demonstrated either by break-apart or by fusion

FISH design. Positive signal patterns have been seen in most secretory breast carcinoma tumour

cells using either assay strategy.

8. Chromosomal translocations mainly associated with colorectal cancer

The first recurrent fusion gene in colorectal cancer was reported in 2011.[98] Bass et al

correlated the genomes of nine colorectal cancers with paired non-neoplastic tissue controls.

Recurrent *VTI1A-TCF7L2* fusion was identified in 3% of colorectal cancers.[98] Their findings

indicated that functionally important fusion events also occur in colorectal cancers, but the

clinical impact of these is yet to be elucidated. RNA-sequencing studies reported by Seshagiri et al identified multiple fusion transcripts in colorectal cancer, including recurrent gene fusions involving R-spondin family members *EIF3E-RSPO2* and *PTPRK-RSPO3* that occurred with a cumulative frequency of 10% in colorectal cancers.[99] Other translocations reported in recent years include *EML4-ALK, C2orf44-ALK*, *SLC34A2-ROS1*, and *NAV2-TCF7L1*.[66]

9. Chromosomal translocations mainly associated with thyroid cancer

More than 10 rearrangements involving *RET* have been reported; all of the rearrangements are formed by fusion of the RET tyrosine kinase domain with a fusion partner gene [100-103]. *RET* rearrangements have been identified almost exclusively in papillary thyroid carcinomas; most frequent were *RET-CCDC6* (60%), *RET-NCOA4* (20%) and *RET- PRKAR1A* (5-12%)[67, 68, 104]. The fusion genes code for constitutively activated proteins driving uncontrolled proliferation of follicular cells.

Kelly et al reported that *STRN-ALK* fusion occurs in a subset of patients with highly aggressive types of thyroid cancer and provide initial evidence suggesting that it may represent a therapeutic target for these patients. STRN-ALK fusion protein leads to constitutive activation of ALK kinase.[105]

Follicular thyroid carcinoma accounts for approximately 20% of all thyroid malignancies. The t(2;3)(q13;p25) translocation, fusion of the thyroid transcription factor, paired box gene 8 (*PAX8*) with peroxisome proliferator activated receptor γ (*PPARG*) is most commonly observed (30%) in follicular thyroid carcinoma.[106] The fusion product acts as an oncogene by

accelerating cellular growth, down-regulating apoptosis, promoting anchorage-independence, and causing loss of contact inhibition. It is noteworthy that rearrangement of these genes has also been identified in benign thyroid adenomas with a break-apart frequency between 3% and 6%.[107, 108]

10. Chromosomal translocations mainly associated with salivary gland tumours

Approximately 20% of salivary gland tumours harbour chromosomal translocation.[109] There are four major recurrent translocations in malignant salivary gland tumours: the *MYB-NFIB* fusion in adenoid cystic carcinoma, the *CRTC1-MAML2* fusion in mucoepidermoid carcinoma, the *ETV6-NTRK3* fusion in mammary analogue secretory carcinoma, and the *EWSR1-ATF1* fusion in hyalinizing clear cell carcinoma (**Table 2**)[96, 97, 110, 111]. The identification of recurrent tumour-specific chromosomal translocations and novel fusion oncogenes has diagnostic, therapeutic, and prognostic implications.

10.1 Pleomorphic adenoma

Pleomorphic adenoma is a benign salivary gland tumour most often arising in the parotid gland. The tumour presents with a highly specific and recurrent pattern of chromosome abnormalities in 70% of cases. There are four cytogenetic categories of pleomorphic adenoma. These involve 8q12 (39%), 12q13-15 (8%), other recurring translocations (23%), and cytogenetically unchanged cases (30%). Of cases with rearrangements, the 8q12 rearrangement [t(3;8)(p21;q12)], represents almost half of the diagnostic translocations found.

10.2 Mucoepidermoid carcinoma

Mucoepidermoid carcinoma represents a distinct type of polymorphous tumour, containing three cellular elements in varying proportions: squamous cells, mucus-secreting cells, and "intermediate" cells. The *CRTC1-MAML2* fusion is present in 55% of mucoepidermoid carcinomas. The fusion oncogene derived from chromosomal translocation that binds cyclic-AMP response element protein related transcription co-factor 1 (*CRTC1*) with mastermind-like 2 NOTCH signaling coactivator (*MAML2*), t(11;19)(q12;p13) is aetiological for some mucoepidermoid carcinomas. When present, this marker confers a favourable survival outcome when compared with fusion-negative tumours.[112]

10.3 Adenoid cystic carcinoma

Recurrent t(6;9)(q22–23;p23–24) translocation in adenoid cystic carcinoma results in a fusion of the *MYB* proto-oncogene with transcription factor gene *NFIB*[113]. *MYB* is a leucine zipper transcription factor at 6q22-24 that participates in the regulation of cell proliferation, apoptosis, and differentiation.[114] West et al used FISH to investigate *MYB* translocation in 37 of these tumors. *MYB-NFIB* translocation was present in 49% of adenoid cystic carcinomas but not in other salivary gland tumours or non-salivary gland neoplasms.[115] A subset of about 20% of adenoid cyst carcinomas lacks any detectable *MYB* gene fusion.[116, 117] The high frequency of this fusion in adenoid cystic carcinoma indicates that the transcript may play a developmental role in a significant subset of these tumours. Therapies directed against *MYB-NFIB* transcriptional targets may improve the prognosis for this chemoresistant neoplasm.

10.4 Mammary analogue secretory carcinoma

Mammary analogue secretory carcinoma (MASC) is a recently recognized salivary gland tumour that is histologically, immunohistochemically, and genetically similar to secretory carcinoma of the breast.[118] MASC harbours a t(12;15) (p13;q25) translocation resulting in fusion of an E-twenty-six family member (*ETV6*) and the neurotrophic tyrosine kinase receptor type 3 (*NTRK3*) gene.[119] Histologically, conventional MASC displays a lobulated growth pattern of a tumour composed of microcystic, tubular, and solid structures. Between epithelial structures, one finds abundant eosinophilic homogenous or bubbly secretions. Majewska et al investigated seven MASC by FISH, and the *ETV6-NTRK3* rearrangement was identified in six cases.[120] For FISH analysis, a dual-colour break-apart probe for the *ETV6* gene exhibits a "split" fluorescent signal in nuclei where the *ETV6* gene participates in translocation. MASC behaves as a low-grade carcinoma with 15–20% recurrence, lymph node metastases in 15–20% of cases, and occasional mortality.[118, 121] *ETV6* FISH is useful to diagnose difficult cases and to exclude the tumours that morphologically mimic MASC.

10.5 Hyalinizing clear cell carcinoma

Hyalinizing clear cell carcinoma (HCCC) is a recently described minor salivary gland tumour composed of glycogen-rich clear cells with hyalinized or myxoid stroma. Gene fusion between Ewing sarcoma breakpoint region 1 (*EWSR1*) and the activating transcription factor 1 (*ATF1*) gene is a relatively consistent finding in hyalinizing clear cell carcinoma.[122] However, EWSR1-ATF1 translocation could also be found in other types of tumour including angiomatoid fibrous histiocytoma, angiosarcoma of the parotid gland, clear cell sarcoma of soft tissue, and clear cell sarcoma-like tumor from the GI tract.[51, 123-126] In one study, the *ATF1* gene

translocation was found in 82% of hyalinizing clear cell carcinoma cases, but in none of the other tumours in the differential diagnosis.[109]

11. Chromosomal translocations mainly associated with Spitz nevi and melanoma

The genetic underpinnings of Spitz nevi are poorly understood, and alterations in melanoma-associated oncogenes are typically absent. Spitzoid neoplasms harbour kinase fusions of *ROS1* (17%), *NTRK1* (16%), *ALK* (10%), *BRAF* (5%), and *RET* (3%) in a mutually exclusive pattern.[127] The chimeric proteins are constitutively activated, which stimulate oncogenic signaling and initiate the tumorigenesis. In a study of 140 spitzoid neoplasms, Wiesner et al and colleagues demonstrated that kinase fusions were present in 18 of 30 Spitz nevi (60%) and within 6 of 8 atypical Spitz tumours (75%). The kinase gene fusions involved *ROS1* (26%, 16/73), *ALK* (11%, 8/75), *NTRK1* (11%, 8/75), *BRAF* (5%, 4/75), and *RET* (3%, 2/75). FISH can be used as an ancillary tool in the diagnosis of ambiguous melanocyte neoplasms, since Spitz nevi are benign and do not require wide excision.[127]

Molecular alterations commonly seen in melanomas are typically absent from Spitz nevi and Spitz nevi contain translocations not usually found in melanoma[91, 128-130]. Translocations involving *BRAF* and *MET* genes have been recently reported in melanoma patients (**Table 2**). *BRAF* fusion genes characteristically activate the MAPK pathway with transformation abilities [131, 132]. This activation of the MAPK pathway renders the tumours potentially sensitive to MEK inhibition.

MET is a high-affinity tyrosine kinase receptor with functions in angiogenesis, cellular motility, growth and invasion.[133] Yeh et al analyzed 1202 equivocal pigmented skin lesions representing spitzoid melanoma, Spitz nevi, conventional nevi, deep penetrating nevus-like lesions and blue nevi. The patients' tumours were tested by comparative genomic hybridization. *MET* translocations were found in six melanocytic tumours resulting in the following fusion genes: *TRIM4-MET, ZKSCAN1-MET, PPFIBP1-MET LRRFIP1-MET, EPS15-MET*, and *DCTN1-MET*.[134] *MET* fusion genes are driven by the promoter of the partner gene and express MET without control.

12. Chromosomal translocations mainly associated with tumours of the central nervous system

The WHO 2016 classification of tumours of the central nervous system emphasizes the importance of molecular classification.[135] More than 10 translocations have been reported in glioblastomas and gene fusions occur in approximately 30-50% of glioblastoma patients (**Table 2**).[136-139] *PTPRZ1-MET* translocation was detected in 15% of glioblastomas in independent cohorts, rendering it the most frequently recurring transcript in glioblastoma. Recently, Bao et al investigated 272 gliomas by RNA seq and identified 67 in-frame fusion transcripts, including three recurrent fusion transcripts: *FGFR3-TACC3*, *RNF213-SLC26A11*,and *PTPRZ1-MET*.[139] Fourteen other rare fusion transcripts containing sequences of genes involved in the canonical glioblastoma signaling pathways were also found.

Co-deletion of 1p/19q has been observed in up to 70% of oligodendrogliomas and 50% of mixed oligoastrocytomas[140-143]. Deletions of 1p and 19q have been associated with prolonged

survival in patients with oligodendrogliomas and mixed oligoastrocytomas. Jenkins et al hypothesized that the majority of 1p and 19q deletions in gliomas were derived from a translocation t(1;19)(q10;p10), which has a prevalence of 81% in all 1p/19q deletion cases.[144]

KIAA1549-BRAF translocations are characteristic of pilocytic astrocytoma.[138, 145] The translocation was found by whole-genome sequencing of 96 pilocytic astrocytomas.[145] These new molecular revelations suggested that *BRAF* targeted therapy may be applicable in pilocytic astrocytomas since the majority of tumours harbour *KIAA1549-BRAF* fusions (**Table 2**).

Ependymoma arises from the ependymal cells of the brain and spinal cord. Surgery and irradiation are the major treatments for this disease since chemotherapy is ineffective in most patients.[146] Parker et al showed that more than two-thirds of supratentorial ependymomas contained chromosomal translocations between avian reticuloendotheliosis viral oncogene homolog A (*RELA*) and chromosome 11 open reading frame 95(*C11orf95*).[147] The resulting fusion protein activates *NF-κB* target genes, transforming the cells.[148] This finding is significant not only for understanding the biology of the tumour but also affords potential for an effective treatment.

13. Conclusions

Over the past decade, FISH analysis of neoplasms has become one of the most rapidly growing areas in genomic medicine and surgical pathology practice. As more diagnostic and treatment algorithms incorporate the results of FISH, demand for the technology will become more widespread. Common FISH-detected alterations are chromosome deletions, gains, translocations,

amplifications, and polysomy. These chromosome alterations may have diagnostic and therapeutic implications for many tumour types. Integrating genomic testing into cancer treatment decisions poses many technical challenges, but rapid progress is being made in overcoming these precision medicine challenges. Next generation sequencing platforms allow detection of fusion genes at both the transcriptional and genomic levels. The rapidly emerging RNA sequencing (RNA-seq) technology has empowered an increasing pace of fusion gene identification. RNA-seq is superior to current molecular test methods in its capacity to detect gene mutations simultaneously, the precise mapping of break-point and joint sequences, and the discovery of cryptic fusions and fusion genes with unknown partners or with short physical distance between the fusion partners. FISH assessment of chromosomal changes is a continuously evolving technology. Its role in clarifying cancer diagnoses and its contributions to the decisions involved in choice of cancer therapy will become ever more important to surgical pathologists and the clinicians and patients they serve.

Figure Legends

Figure 1 Break-apart probe design for translocations with multiple fusion partners. A break-apart probe set is composed of two probes specific for loci physically close to each other on the chromosome in their wild type configuration. The wild type signal pattern shows 2 pairs of closely approximated or fused signals (A). When translocation occurs involving a breakpoint between the two probe sites, the originally juxtaposed loci (fusion signals) split apart (B). The beauty of this design is that it detects chromosomal translocation regardless of the fusion partner involved. However, the break-apart probe only identifies the breaking away of a gene fragment from its original location. It does not determine which chromosome receives the fragment or which genes may serve as fusion partners in the new location.

Figure 2 Fusion design for translocation between specific partners. A fusion probe set contains two locus-specific probes labeled with different colours targeting the genes known to fuse in certain tumours or diseases. The fusion probes identify chromosomal loci far from each other either on the same chromosome or on different chromosomes. The wild type configuration shows two separated signals resulting from physically separated chromosome loci (A). When fusion occurs, the two probes move to a closely approximated position (fusion signal, B). This provides direct evidence of a gene fusion with definitive fusion partners identified.

Figure 3 Signal patterns of ALK split-apart probes. The commonly used *ALK* split-apart FISH test uses dual colour labeled probes covering the *ALK* gene (yellow) and 3' flanking region of *ALK* (red). When translocation occurs, the normal closely approximated signal pattern separates into distinct yellow and red signals (in commercial FISH ALK translocation kits Green and Red

signals may be used). Since *ALK* translocations involve multiple fusion partners, a split-apart

design ensures that the probe set will uncover *ALK* translocations with most of the possible

fusion partners.

Figure 4 Genomic translocation relationships presented by Circos plot. Circos applies a circular

ideogram displaying relationships between genomic intervals. The Circos plot is a ring

composed of all chromosomes in proportionate size clockwise from 1 to Y. This graphic

representation is used to visualize chromosomal translocations associated with a clinical entity.

A specific translocation is shown with a line connecting the two chromosome partner loci

involved in each translocation. The chromosomal translocations that may be involved in Xp11

translocation renal cell carcinomas are shown in A, including inv(X)(p11.2;q12) [*NonO-TFE3*]

(Red), t(X;1)(p11.2;p34) [*PSF-TEF3*] (Gray), t(X;1)(p11.2;q21) [*PRCC-TFE3*] (Blue),

t(X;3)(p11.2;q23) [*unknown-TFE3*] (Black), t(X;10)(p11.2;q23) [*unknown-TFE3*] (Yellow),

t(X;17)(p11.2;q23) [*CLTC-TFE3*] (Magenta), t(X;17)(p11.2;q25) [*ASPL-TFE3*] (Green),

t(X;19)(p11.2;q13.1) [*unknown-TFE3*] (Purple). Translocations involved in *TFEB* translocation

renal cell carcinoma are shown in B, t(6;11)(p21;q13) [*MALAT1-TFEB*] (Blue), t(6;17)(p21;q25)

[*ASPSCR1-TFEB*] (Red).

Figure 5 Signal patterns of *TFE3* split-apart probes. Renal cell carcinomas associated with

Xp11.2 translocation involve several different translocations resulting in gene fusions of the

TFE3 gene with various fusion partners. The break-apart FISH assay uses probes both upstream

(yellow) and downstream (red) to *TFE3* showing different signal patterns in female (A) and male

(B) patients. A positive result in a female patient shows a fused or closely approximated normal

yellow-red signal pair (uninvolved X chromosome) and either a pair of split-apart signals or a

single yellow or red signal due to section truncation artifact. Because males have only one X-

chromosome, a positive result in a male patient consists either of a pair of split-apart yellow and

red signals, or of a single yellow or red signal due to section truncation.

Figure 6 Signal patterns of *TMPRSS2-ERG* translocation by tri-colour split-apart probes. The

TMPRSS2-ERG tri-colour fused probe uses 3 different colour probes recognizing the up-stream

end of *TMPRSS2* (orange), and both up- and down- stream ends of *ERG* (yellow, red),

respectively. The probes hybridizing to the wild type *TMPRSS2/ERG* loci show the normal co-

localized red-yellow-orange pattern (A). *TMPRSS2/ERG* loci rearrangement via breaks in both

ERG and *TMPRSS2* genes leads to a red-orange fusion of *ERG* down-stream signal to the

TMPRSS2 signal. The *ERG* up-stream signal may either split from the down-stream sequence as

in (B), or be deleted entirely as shown with the signal pattern shown in (C).

References:

1. Buongiorno-Nardelli M, Amaldi F. Autoradiographic detection of molecular hybrids between RNA and DNA in tissue sections. *Nature* 1970;**225**:946-948.

2. John HA, Birnstiel ML, Jones KW. RNA-DNA hybrids at the cytological level. *Nature* 1969;**223**:582-587.

3. Gall JG, Pardue ML. Formation and detection of RNA-DNA hybrid molecules in cytological preparations. *Proc Natl Acad Sci U S A* 1969;**63**:378-383.

4. Katsanis SH, Katsanis N. Molecular genetic testing and the future of clinical genomics. *Nat Rev Genet* 2013;**14**:415-426.

5. Cheng L, Zhang DY, Eble JN. Molecular Genetic Pathology. 2nd ed. New York, NY: Springer, 2013.

6. Cheng L, Eble JN. Molecular Surgical Pathology. 1st ed. New York, NY: Springer, 2013.

7. Mitelman F, Johansson B, Mertens F. Fusion genes and rearranged genes as a linear function of chromosome aberrations in cancer. *Nat Genet* 2004;**36**:331-334.

8. Lin C, Yang L, Tanasa B, *et al.* Nuclear receptor-induced chromosomal proximity and DNA breaks underlie specific translocations in cancer. *Cell* 2009;**139**:1069-1083.

9. Doroshow JH, Kummar S. Translational research in oncology--10 years of progress and future prospects. *Nat Rev Clin Oncol* 2014;**11**:649-662.

10. Mertens F, Johansson B, Fioretos T*, et al.* The emerging complexity of gene fusions in cancer. *Nat Rev Cancer* 2015;**15**:371-381.

11. Martin CL, Warburton D. Detection of chromosomal aberrations in clinical practice: from karyotype to genome sequence. *Annu Rev Genomics Hum Genet* 2015;**16**:309-326.

2.   Selvarajah S, Pyne S, Chen E*, et al.* High-resolution array CGH and gene expression profiling of alveolar soft part sarcoma. *Clin Cancer Res* 2014;**20**:1521-1530.

3.   Friedman AA, Letai A, Fisher DE*, et al.* Precision medicine for cancer with next-generation functional diagnostics. *Nat Rev Cancer* 2015;**15**:747-756.

4.   Kumar-Sinha C, Kalyana-Sundaram S, Chinnaiyan AM. Landscape of gene fusions in epithelial cancers: seq and ye shall find. *Genome Med* 2015;**7**:129.

5.   Cheng L, Zhang S, MacLennan GT*, et al.* Laser-assisted microdissection in translational research: theory, technical considerations, and future applications. *Appl Immunohistochem Mol Morphol* 2013;**21**:31-47.

6.   Roukos V, Misteli T. The biogenesis of chromosome translocations. *Nat Cell Biol* 2014;**16**:293-300.

7.   Bunting SF, Nussenzweig A. End-joining, translocations and cancer. *Nat Rev Cancer* 2013;**13**:443-454.

8.   Vorsanova SG, Yurov YB, Iourov IY. Human interphase chromosomes: a review of available molecular cytogenetic technologies. *Mol Cytogenet* 2010;**3**:1.

9.   Speicher MR, Carter NP. The new cytogenetics: blurring the boundaries with molecular biology. *Nat Rev Genet* 2005;**6**:782-792.

0.   Cui C, Shu W, Li P. Fluorescence In situ Hybridization: Cell-Based Genetic Diagnostic and Research Applications. *Front Cell Dev Biol* 2016;**4**:89.

1.   Byron SA, Van Keuren-Jensen KR, Engelthaler DM*, et al.* Translating RNA sequencing into clinical diagnostics: opportunities and challenges. *Nat Rev Genet* 2016;**17**:257-271.

2.   Goodwin S, McPherson JD, McCombie WR. Coming of age: ten years of next-generation sequencing technologies. *Nat Rev Genet* 2016;**17**:333-351.

3. Martin JA, Wang Z. Next-generation transcriptome assembly. *Nat Rev Genet* 2011;**12**:671-682.

4. Yoshihara K, Wang Q, Torres-Garcia W*, et al.* The landscape and therapeutic relevance of cancer-associated transcript fusions. *Oncogene* 2015;**34**:4845-4854.

5. Latysheva NS, Babu MM. Discovering and understanding oncogenic gene fusions through data intensive computational approaches. *Nucleic Acids Res* 2016.

6. Ozsolak F, Milos PM. RNA sequencing: advances, challenges and opportunities. *Nat Rev Genet* 2011;**12**:87-98.

7. Mertens F, Antonescu CR, Mitelman F. Gene fusions in soft tissue tumors: Recurrent and overlapping pathogenetic themes. *Genes Chromosomes Cancer* 2016;**55**:291-310.

8. Flechter CDM, Bridge JA, Hogendoom PCW*, et al.* WHO Classification of tumours of soft tissue and bone. Lyon, France International Agency for Research on Cancer (IARC) Press 2013.

9. Fletcher CD. The evolving classification of soft tissue tumours - an update based on the new 2013 WHO classification. *Histopathology* 2014;**64**:2-11.

0. Thway K, Fisher C. Tumors with EWSR1-CREB1 and EWSR1-ATF1 fusions: The current status. *Am J Surg Pathol* 2012;**36**:e1-e11.

1. Grunewald TG, Bernard V, Gilardi-Hebenstreit P*, et al.* Chimeric EWSR1-FLI1 regulates the Ewing sarcoma susceptibility gene EGR2 via a GGAA microsatellite. *Nat Genet* 2015;**47**:1073-1078.

2. Nielsen TO, Poulin NM, Ladanyi M. Synovial sarcoma: Recent discoveries as a roadmap to new avenues for therapy. *Cancer Discov* 2015;**5**:124-134.

34

3.   Svejstrup JQ. Synovial sarcoma mechanisms: A series of unfortunate events. *Cell*

2013;**153**:11-12.

4.   Chmielecki J, Crago AM, Rosenberg M*, et al.* Whole-exome sequencing identifies a

recurrent NAB2-STAT6 fusion in solitary fibrous tumors. *Nat Genet* 2013;**45**:131-132.

5.   Robinson DR, Wu YM, Kalyana-Sundaram S*, et al.* Identification of recurrent NAB2-

STAT6 gene fusions in solitary fibrous tumor by integrative sequencing. *Nat Genet*

2013;**45**:180-185.

6.   Kouba E, Simper NB, Chen S*, et al.* Solitary fibrous tumour of the genitourinary tract: a

clinicopathological study of 11 cases and their association with the NAB2-STAT6 fusion

gene. *J Clin Pathol* 2016.

7.   Mohajeri A, Tayebwa J, Collin A*, et al.* Comprehensive genetic analysis identifies a

pathognomonic NAB2/STAT6 fusion gene, nonrandom secondary genomic imbalances,

and a characteristic gene expression profile in solitary fibrous tumor. *Genes Chromosomes

Cancer* 2013;**52**:873-886.

8.   Gambarotti M, Benini S, Gamberi G*, et al.* CIC-DUX4 Fusion-positive round cell

sarcomas of soft tissue and bone: a single institution morphologic and molecular analysis

of 7 cases. *Histopathology* 2016.

9.   Choi EY, Thomas DG, McHugh JB*, et al.* Undifferentiated small round cell sarcoma with

t(4;19)(q35;q13.1) CIC-DUX4 fusion: a novel highly aggressive soft tissue tumor with

distinctive histopathology. *Am J Surg Pathol* 2013;**37**:1379-1386.

0.   Choi E, Williamson SR, Montironi R*, et al.* Inflammatory myofibroblastic tumour of the

urinary bladder: the role of immunoglobulin G4 and the comparison of two

35

immunohistochemical antibodies and fluorescence in-situ hybridization for the detection of anaplastic lymphoma kinase alterations. *Histopathology* 2015;**67**:20-38.

1. Mano H. ALKoma: a cancer subtype with a shared target. *Cancer Discov* 2012;**2**:495-502.

2. Hallberg B, Palmer RH. Mechanistic insight into ALK receptor tyrosine kinase in human cancer biology. *Nat Rev Cancer* 2013;**13**:685-700.

3. Butrynski JE, D'Adamo DR, Hornick JL*, et al.* Crizotinib in ALK-rearranged inflammatory myofibroblastic tumor. *N Engl J Med* 2010;**363**:1727-1733.

4. Gaudichon J, Jeanne-Pasquier C, Deparis M*, et al.* Complete and repeated response of a metastatic ALK-rearranged inflammatory myofibroblastic tumor to Crizotinib in a teenage girl. *J Pediatr Hematol Oncol* 2016;**38**:308-311.

5. Yamamoto H, Yoshida A, Taguchi K*, et al.* ALK, ROS1 and NTRK3 gene rearrangements in inflammatory myofibroblastic tumours. *Histopathology* 2016;**69**:72-83.

6. Antonescu CR, Suurmeijer AJ, Zhang L*, et al.* Molecular characterization of inflammatory myofibroblastic tumors with frequent ALK and ROS1 gene fusions and rare novel RET rearrangement. *Am J Surg Pathol* 2015;**39**:957-967.

7. Hodge JC, Pearce KE, Wang X*, et al.* Molecular cytogenetic analysis for TFE3 rearrangement in Xp11.2 renal cell carcinoma and alveolar soft part sarcoma: validation and clinical experience with 75 cases. *Mod Pathol* 2014;**27**:113-127.

8. Brown RE, Buryanek J, Katz AM*, et al.* Alveolar rhabdomyosarcoma: morphoproteomics and personalized tumor graft testing further define the biology of PAX3-FKHR(FOXO1) subtype and provide targeted therapeutic options. *Oncotarget* 2016;**7**:46263-46272.

9.   Thway K, Rockcliffe S, Gonzalez D*, et al.* Utility of sarcoma-specific fusion gene analysis in paraffin-embedded material for routine diagnosis at a specialist centre. *J Clin Pathol* 2010;**63**:508-512.

0.   Wang WL, Mayordomo E, Zhang W*, et al.* Detection and characterization of EWSR1/ATF1 and EWSR1/CREB1 chimeric transcripts in clear cell sarcoma (melanoma of soft parts). *Mod Pathol* 2009;**22**:1201-1209.

1.   Hisaoka M, Ishida T, Kuo TT*, et al.* Clear cell sarcoma of soft tissue: A clinicopathologic, immunohistochemical, and molecular analysis of 33 cases. *Am J Surg Pathol* 2008;**32**:452-460.

2.   Shaw AT, Engelman JA. ALK in lung cancer: Past, present, and future. *J Clin Oncol* 2013;**31**:1105-1111.

3.   Cheng L, Alexander RE, Maclennan GT*, et al.* Molecular pathology of lung cancer: Key to personalized medicine. *Mod Pathol* 2012;**25**:347-369.

4.   Swanton C, Govindan R. Clinical implications of genomic discoveries in lung cancer. *N Engl J Med* 2016;**374**:1864-1873.

5.   Hirsch FR, Scagliotti GV, Mulshine JL*, et al.* Lung cancer: Current therapies and new targeted treatments. *Lancet* 2016.

6.   Alkan A, Koksoy EB, Utkan G. First-line crizotinib in ALK-positive lung cancer. *N Engl J Med* 2015;**372**:781-782.

7.   Shen L, Ji HF. Ceritinib in ALK-rearranged non-small-cell lung cancer. *N Engl J Med* 2014;**370**:2537.

8.   Morton MJ, Zhang S, Lopez-Beltran A*, et al.* Telomere shortening and chromosomal abnormalities in intestinal metaplasia of the urinary bladder. *Clin Cancer Res* 2007;**13**:6232-6236.

9.   Bergethon K, Shaw AT, Ou SH*, et al.* ROS1 rearrangements define a unique molecular class of lung cancers. *J Clin Oncol* 2012;**30**:863-870.

0.   Uguen A, De Braekeleer M. ROS1 fusions in cancer: A review. *Future Oncol* 2016;**12**:1911-1928.

1.   Takeuchi K, Soda M, Togashi Y*, et al.* RET, ROS1 and ALK fusions in lung cancer. *Nat Med* 2012;**18**:378-381.

2.   Charest A, Lane K, McMahon K*, et al.* Fusion of FIG to the receptor tyrosine kinase ROS in a glioblastoma with an interstitial del(6)(q21q21). *Genes Chromosomes Cancer* 2003;**37**:58-71.

3.   Davies KD, Doebele RC. Molecular pathways: ROS1 fusion proteins in cancer. *Clin Cancer Res* 2013;**19**:4040-4045.

4.   Gu TL, Deng X, Huang F*, et al.* Survey of tyrosine kinase signaling reveals ROS kinase fusions in human cholangiocarcinoma. *PLoS One* 2011;**6**:e15640.

5.   Lee J, Lee SE, Kang SY*, et al.* Identification of ROS1 rearrangement in gastric adenocarcinoma. *Cancer* 2013;**119**:1627-1635.

6.   Aisner DL, Nguyen TT, Paskulin DD*, et al.* ROS1 and ALK fusions in colorectal cancer, with evidence of intratumoral heterogeneity for molecular drivers. *Mol Cancer Res* 2014;**12**:111-118.

7.   Mulligan LM. RET revisited: Expanding the oncogenic portfolio. *Nat Rev Cancer* 2014;**14**:173-186.

8.   Shaw AT, Hsu PP, Awad MM, *et al.* Tyrosine kinase gene rearrangements in epithelial

     malignancies. *Nat Rev Cancer* 2013;**13**:772-787.

9.   Vargas AJ, Harris CC. Biomarker development in the precision medicine era: lung cancer

     as a case study. *Nat Rev Cancer* 2016;**16**:525-537.

0.   Wang R, Hu H, Pan Y, *et al.* RET fusions define a unique molecular and clinicopathologic

     subtype of non-small-cell lung cancer. *J Clin Oncol* 2012;**30**:4352-4359.

1.   Drilon A, Wang L, Hasanovic A, *et al.* Response to Cabozantinib in patients with RET

     fusion-positive lung adenocarcinomas. *Cancer Discov* 2013;**3**:630-635.

2.   Travis WD, Brambilla E, Burke A, *et al.* WHO classification of tumours of the lung,

     pleura, thymus and heart. 4th ed. Lyon, France: International Agency for Research on

     Cancer (IARC) Press, 2015.

3.   Thway K, Nicholson AG, Lawson K, *et al.* Primary pulmonary myxoid sarcoma with

     EWSR1-CREB1 fusion: a new tumor entity. *Am J Surg Pathol* 2011;**35**:1722-1732.

4.   Moch H, Humphrey PA, Ulbright TM, *et al.* WHO Classification of Tumors of the Uronary

     System and Male Genital Organ. 4th ed. Lyon, France: International Agency for Research

     on Cancer (IARC) Press, 2016.

5.   Smith NE, Illei PB, Allaf M, *et al.* t(6;11) renal cell carcinoma (RCC): Expanded

     immunohistochemical profile emphasizing novel RCC markers and report of 10 new

     genetically confirmed cases. *Am J Surg Pathol* 2014;**38**:604-614.

6.   Kauffman EC, Ricketts CJ, Rais-Bahrami S, *et al.* Molecular genetics and cellular features

     of TFE3 and TFEB fusion kidney cancers. *Nat Rev Urol* 2014;**11**:465-475.

7.   Argani P. MiT family translocation renal cell carcinoma. *Semin Diagn Pathol* 2015;**32**:103-

     113.

8.   Argani P, Zhong M, Reuter VE, *et al.* TFE3-fusion variant analysis defines specific clinicopathologic associations among Xp11 translocation cancers. *Am J Surg Pathol* 2016;**40**:723-737.

9.   Rao Q, Williamson SR, Zhang S, *et al.* TFE3 greak-apart FISH has a higher sensitivity for Xp11.2 translocation-associated renal cell carcinoma compared with TFE3 or cathepsin K immunohistochemical staining alone: Expanding the morphologic spectrum. *Am J Surg Pathol* 2013;**37**:804-815.

0.   Malouf GG, Su X, Yao H, *et al.* Next-generation sequencing of translocation renal cell carcinoma reveals novel RNA splicing partners and frequent mutations of chromatin-remodeling genes. *Clin Cancer Res* 2014;**20**:4129-4140.

1.   Rao Q, Liu B, Cheng L, *et al.* Renal cell carcinomas with t(6;11)(p21;q12): A clinicopathologic study emphasizing unusual morphology, novel alpha-TFEB gene fusion point, immunobiomarkers, and ultrastructural features, as well as detection of the gene fusion by fluorescence in situ hybridization. *Am J Surg Pathol* 2012;**36**:1327-1338.

2.   Lopez-Beltran A, Cheng L, Raspollini MR, *et al.* SMARCB1/INI1 genetic alterations in renal medullary carcinomas. *Eur Urol* 2016;**69**:1062-1064.

3.   Cheng JX, Tretiakova M, Gong C, *et al.* Renal medullary carcinoma: Rhabdoid features and the absence of INI1 expression as markers of aggressive behavior. *Mod Pathol* 2008;**21**:647-652.

4.   Calderaro J, Masliah-Planchon J, Richer W, *et al.* Balanced translocations disrupting SMARCB1 are hallmark recurrent genetic alterations in renal medullary carcinomas. *Eur Urol* 2016;**69**:1055-1061.

5.   Marino-Enriquez A, Ou WB, Weldon CB, *et al.* ALK rearrangement in sickle cell trait-associated renal medullary carcinoma. *Genes Chromosomes Cancer* 2011;**50**:146-153.

6.   Sukov WR, Hodge JC, Lohse CM, *et al.* ALK alterations in adult renal cell carcinoma: frequency, clinicopathologic features and outcome in a large series of consecutively treated patients. *Mod Pathol* 2012;**25**:1516-1525.

7.   Kusano H, Togashi Y, Akiba J, *et al.* Two cases of renal cell carcinoma harboring a novel STRN-ALK fusion gene. *Am J Surg Pathol* 2016;**40**:761-769.

8.   Tomlins SA, Rhodes DR, Perner S, *et al.* Recurrent fusion of TMPRSS2 and ETS transcription factor genes in prostate cancer. *Science* 2005;**310**:644-648.

9.   Tomlins SA, Laxman B, Dhanasekaran SM, *et al.* Distinct classes of chromosomal rearrangements create oncogenic ETS gene fusions in prostate cancer. *Nature* 2007;**448**:595-599.

0.   Tomlins SA, Bjartell A, Chinnaiyan AM, *et al.* ETS gene fusions in prostate cancer: from discovery to daily clinical practice. *Eur Urol* 2009;**56**:275-286.

1.   Palanisamy N, Ateeq B, Kalyana-Sundaram S, *et al.* Rearrangements of the RAF kinase pathway in prostate cancer, gastric cancer and melanoma. *Nat Med* 2010;**16**:793-798.

2.   Yoshimoto M, Joshua AM, Chilton-Macneill S, *et al.* Three-color FISH analysis of TMPRSS2/ERG fusions in prostate cancer indicates that genomic microdeletion of chromosome 21 is associated with rearrangement. *Neoplasia* 2006;**8**:465-469.

3.   Fisher KW, Zhang S, Wang M, *et al.* TMPRSS2-ERG gene fusion is rare compared to PTEN deletions in stage T1a prostate cancer. *Mol Carcinog* 2016.

4.   Williamson SR, Zhang S, Yao JL, *et al.* ERG-TMPRSS2 rearrangement is shared by concurrent prostatic adenocarcinoma and prostatic small cell carcinoma and absent in

small cell carcinoma of the urinary bladder: evidence supporting monoclonal origin. *Mod Pathol* 2011;**24**:1120-1127.

5. Li Z, Tognon CE, Godinho FJ*, et al.* ETV6-NTRK3 fusion oncogene initiates breast cancer from committed mammary progenitors via activation of AP1 complex. *Cancer Cell* 2007;**12**:542-558.

6. Del Castillo M, Chibon F, Arnould L*, et al.* Secretory breast carcinoma: A histopathologic and genomic spectrum characterized by a joint specific ETV6-NTRK3 gene fusion. *Am J Surg Pathol* 2015;**39**:1458-1467.

7. Tognon C, Knezevich SR, Huntsman D*, et al.* Expression of the ETV6-NTRK3 gene fusion as a primary event in human secretory breast carcinoma. *Cancer Cell* 2002;**2**:367-376.

8. Bass AJ, Lawrence MS, Brace LE*, et al.* Genomic sequencing of colorectal adenocarcinomas identifies a recurrent VTI1A-TCF7L2 fusion. *Nat Genet* 2011;**43**:964-968.

9. Seshagiri S, Stawiski EW, Durinck S*, et al.* Recurrent R-spondin fusions in colon cancer. *Nature* 2012;**488**:660-664.

00. Xing M. Molecular pathogenesis and mechanisms of thyroid cancer. *Nat Rev Cancer* 2013;**13**:184-199.

01. Cabanillas ME, McFadden DG, Durante C. Thyroid cancer. *Lancet* 2016.

02. Cancer Genome Atlas Research Network. Integrated genomic characterization of papillary thyroid carcinoma. *Cell* 2014;**159**:676-690.

03. Nikiforov YE, Nikiforova MN. Molecular genetics and diagnosis of thyroid cancer. *Nat Rev Endocrinol* 2011;**7**:569-580.

04.　Romei C, Ciampi R, Elisei R. A comprehensive overview of the role of the RET proto-oncogene in thyroid carcinoma. *Nat Rev Endocrinol* 2016;**12**:192-202.

05.　Kelly LM, Barila G, Liu P*, et al.* Identification of the transforming STRN-ALK fusion as a potential therapeutic target in the aggressive forms of thyroid cancer. *Proc Natl Acad Sci U S A* 2014;**111**:4233-4238.

06.　Raman P, Koenig RJ. Pax-8-PPAR-gamma fusion protein in thyroid carcinoma. *Nat Rev Endocrinol* 2014;**10**:616-623.

07.　Caria P, Frau DV, Dettori T*, et al.* Optimizing detection of RET and PPARg rearrangements in thyroid neoplastic cells using a home-brew tetracolor probe. *Cancer Cytopathol* 2014;**122**:377-385.

08.　Sharifah NA, Zakaria Z, Chia WK. FISH analysis using PPAR gamma-specific probes for detection of PAX8-PPAR gamma translocation in follicular thyroid neoplasms. *Methods Mol Biol* 2013;**952**:187-196.

09.　Weinreb I. Translocation-associated salivary gland tumors: a review and update. *Adv Anat Pathol* 2013;**20**:367-377.

10.　Amelio AL, Fallahi M, Schaub FX*, et al.* CRTC1/MAML2 gain-of-function interactions with MYC create a gene signature predictive of cancers with CREB-MYC involvement. *Proc Natl Acad Sci U S A* 2014;**111**:E3260-3268.

11.　Tonon G, Modi S, Wu L*, et al.* t(11;19)(q21;p13) translocation in mucoepidermoid carcinoma creates a novel fusion product that disrupts a notch signaling pathway. *Nat Genet* 2003;**33**:208-213.

12.   Anzick SL, Chen WD, Park Y, *et al.* Unfavorable prognosis of CRTC1-MAML2 positive mucoepidermoid tumors with CDKN2A deletions. *Genes Chromosomes Cancer* 2010;**49**:59-69.

13.   Wysocki PT, Izumchenko E, Meir J, *et al.* Adenoid cystic carcinoma: emerging role of translocations and gene fusions. *Oncotarget* 2016.

14.   Ramsay RG, Gonda TJ. MYB function in normal and cancer cells. *Nat Rev Cancer* 2008;**8**:523-534.

15.   West RB, Kong C, Clarke N, *et al.* MYB expression and translocation in adenoid cystic carcinomas and other salivary gland tumors with clinicopathologic correlation. *Am J Surg Pathol* 2011;**35**:92-99.

16.   Stenman G, Persson F, Andersson MK. Diagnostic and therapeutic implications of new molecular biomarkers in salivary gland cancers. *Oral Oncol* 2014;**50**:683-690.

17.   North JP, Garrido MC, Kolaitis NA, *et al.* Fluorescence in situ hybridization as an ancillary tool in the diagnosis of ambiguous melanocytic neoplasms: a review of 804 cases. *Am J Surg Pathol* 2014;**38**:824-831.

18.   Skalova A, Vanecek T, Sima R, *et al.* Mammary analogue secretory carcinoma of salivary glands, containing the ETV6-NTRK3 fusion gene: A hitherto undescribed salivary gland tumor entity. *Am J Surg Pathol* 2010;**34**:599-608.

19.   Skalova A, Weinreb I, Hyrcza M, *et al.* Clear cell myoepithelial carcinoma of salivary glands showing EWSR1 rearrangement: Molecular analysis of 94 salivary gland carcinomas with prominent clear cell component. *Am J Surg Pathol* 2015;**39**:338-348.

44

20. Majewska H, Skalova A, Stodulski D, *et al.* Mammary analogue secretory carcinoma of salivary glands: A new entity associated with ETV6 gene rearrangement. *Virchows Arch* 2015;**466**:245-254.

21. Connor A, Perez-Ordonez B, Shago M, *et al.* Mammary analog secretory carcinoma of salivary gland origin with the ETV6 gene rearrangement by FISH: Expanded morphologic and immunohistochemical spectrum of a recently described entity. *Am J Surg Pathol* 2012;**36**:27-34.

22. Antonescu CR, Katabi N, Zhang L, *et al.* EWSR1-ATF1 fusion is a novel and consistent finding in hyalinizing clear-cell carcinoma of salivary gland. *Genes Chromosomes Cancer* 2011;**50**:559-570.

23. Kao YC, Lan J, Tai HC, *et al.* Angiomatoid fibrous histiocytoma: Clinicopathological and molecular characterisation with emphasis on variant histomorphology. *J Clin Pathol* 2014;**67**:210-215.

24. Gru AA, Becker N, Pfeifer JD. Angiosarcoma of the parotid gland with a t(12;22) translocation creating a EWSR1-ATF1 fusion: A diagnostic dilemma. *J Clin Pathol* 2013;**66**:452-454.

25. Hallor KH, Mertens F, Jin Y, *et al.* Fusion of the EWSR1 and ATF1 genes without expression of the MITF-M transcript in angiomatoid fibrous histiocytoma. *Genes Chromosomes Cancer* 2005;**44**:97-102.

26. Wang J, Thway K. Clear cell sarcoma-like tumor of the gastrointestinal tract: An evolving entity. *Arch Pathol Lab Med* 2015;**139**:407-412.

27. Wiesner T, He J, Yelensky R, *et al.* Kinase fusions are frequent in Spitz tumours and spitzoid melanomas. *Nat Commun* 2014;**5**:3116.

45

28. Bradish JR, Cheng L. Molecular pathology of malignant melanoma: changing the clinical practice paradigm toward a personalized approach. *Hum Pathol* 2014;**45**:1315-1326.

29. Cancer Genome Atlas Research Network. Genomic classification of cutaneous melanoma. *Cell* 2015;**161**:1681-1696.

30. Shain AH, Bastian BC. From melanocytes to melanomas. *Nat Rev Cancer* 2016;**16**:345-358.

31. Hutchinson KE, Lipson D, Stephens PJ*, et al.* BRAF fusions define a distinct molecular subset of melanomas with potential sensitivity to MEK inhibition. *Clin Cancer Res* 2013;**19**:6696-6702.

32. Ross JS, Wang K, Chmielecki J*, et al.* The distribution of BRAF gene fusions in solid tumors and response to targeted therapy. *Int J Cancer* 2016;**138**:881-890.

33. Bottaro DP, Rubin JS, Faletto DL*, et al.* Identification of the hepatocyte growth factor receptor as the c-met proto-oncogene product. *Science* 1991;**251**:802-804.

34. Yeh I, Botton T, Talevich E*, et al.* Activating MET kinase rearrangements in melanoma and Spitz tumours. *Nat Commun* 2015;**6**:7174.

35. Louis D, Ohgaki H, Wiestler O*, et al.* WHO Classification of Tumours of the Central Nervous System. 4th ed. Lyon, France: Inernational Agency for Research on Cancer (IARC), 2016.

36. Shah N, Lankerovich M, Lee H*, et al.* Exploration of the gene fusion landscape of glioblastoma using transcriptome sequencing and copy number data. *BMC Genomics* 2013;**14**:818.

37. Frattini V, Trifonov V, Chan JM*, et al.* The integrated landscape of driver genomic alterations in glioblastoma. *Nat Genet* 2013;**45**:1141-1149.

38.   Ceccarelli M, Barthel FP, Malta TM, *et al.* Molecular profiling reveals biologically discrete subsets and pathways of progression in diffuse glioma. *Cell* 2016;**164**:550-563.

39.   Bao ZS, Chen HM, Yang MY, *et al.* RNA-seq of 272 gliomas revealed a novel, recurrent PTPRZ1-MET fusion transcript in secondary glioblastomas. *Genome Res* 2014;**24**:1765-1773.

40.   Eckel-Passow JE, Lachance DH, Molinaro AM, *et al.* Glioma groups based on 1p/19q, IDH, and TERT promoter mutations in tumors. *N Engl J Med* 2015;**372**:2499-2508.

41.   Mur P, Mollejo M, Hernandez-Iglesias T, *et al.* Molecular classification defines 4 prognostically distinct glioma groups irrespective of diagnosis and grade. *J Neuropathol Exp Neurol* 2015;**74**:241-249.

42.   Wesseling P, van den Bent M, Perry A. Oligodendroglioma: Pathology, molecular mechanisms and markers. *Acta Neuropathol* 2015;**129**:809-827.

43.   Rodriguez FJ, Vizcaino MA, Lin MT. Recent advances on the molecular pathology of glial neoplasms in children and adults. *J Mol Diagn* 2016;**18**:620-634.

44.   Jenkins RB, Blair H, Ballman KV, *et al.* A t(1;19)(q10;p10) mediates the combined deletions of 1p and 19q and predicts a better prognosis of patients with oligodendroglioma. *Cancer Res* 2006;**66**:9852-9861.

45.   Jones DT, Hutter B, Jager N, *et al.* Recurrent somatic alterations of FGFR1 and NTRK2 in pilocytic astrocytoma. *Nat Genet* 2013;**45**:927-932.

46.   Merchant TE, Li C, Xiong X, *et al.* Conformal radiotherapy after surgery for paediatric ependymoma: a prospective study. *Lancet Oncol* 2009;**10**:258-266.

47.   Parker M, Mohankumar KM, Punchihewa C, *et al.* C11orf95-RELA fusions drive oncogenic NF-kappaB signalling in ependymoma. *Nature* 2014;**506**:451-455.

148.   Versteeg R. Cancer: Tumours outside the mutation box. *Nature* 2014;**506**:438-439.

Supplementary Material - None

Table 1 Chromosome alterations in mesenchymal and uncertain derivation solid tumours

Tumour Type	Chromosomal Translocation	Genes Involved	%
Adipocytic tumours			
Chondroid lipoma	t(11;16)(q13;p13)	*C11orf95-MKL2*	75-85
Lipoma	t(3;12)(q27;q14)	*HMGA2-LPP*	20–25
	t(12;13)(q13;q14)	*HMGA2-LHFP*	*
	t(3;13)(q27;q14)	*LPP-LHFP*	*
	t(Y;12)(q12;q14)	*?-HMGA2*	*
Lipoblastoma	t(2;8)(q31;q12)	*COL3A1-PLAG1*	50-75
	t(8;8)(q24;q12)	*HAS2-PLAG1*	*
	t(7;8)(q21;q12)	*COL1A2-PLAG1*	*
	t(8;14)(q12;q24)	*RAD51B-PLAG1*	*
Spindle cell/ pleomorphic lipoma	- 13/del(13)(q14)	*RB1*	40–48
	del(16)(q13)	-	40–50
Hibernoma	del(11)(q13-21)	*MEN1*	66–80
Atypical lipomatous tumour/well differentiated liposarcoma	amp(12)(q14-15)	*MDM2*	80–90
	Supernumerary ring	-	75–90
Myxoid liposarcoma	t(12;16)(q13;p11)	*FUS-DDIT3*	90–95
	del(10)(q23)	*PTEN*	7–12
	t(12;22)(q13;q12)	*EWSR1-DDIT3*	*
	t(12;22;20)(q13;q12;q11)	*EWSR1-DDIT3*	*
Fibroblastic/myofibroblastic tumours			
Nodular fasciitis	t(17;22)(p13;q13)	*MYH9-USP6*	90–92
Elastofibroma	amp(X)(q12-q22)	-	16–30
Fibroma of tendon sheath	t(2;11)(q31;q12)	-	#
	t(9;11)(p24;q13)	-	#
Desmoplastic fibroblastoma	t(2;11)(q31;q12)	-	#
	t(11;17)(q12;p11)	-	#
Cellular angiofibroma	del(13)(q14)	*RB1, FOXO1*	54–80
Mammary-type myofibroblastoma	del(13)(q14)	*RB1, FOXO1*	70-92
Tenosynovial giant cell tumour	t(1;2)(p13;q37)	*CSF1-COL6A3*	50–80
Giant cell fibroblastoma	t(17;22)(q22;q13)	*COL1A1-PDGFB*	80–92
Dermatofibrosarcoma protuberans	t(17;22)(q22;q13)	*COL1A1-PDGFB*	74–90
	Supernumerary ring	-	50–65

Inflammatory myofibroblastic tumour	t(1;2)(q21;p23)	*TPM3-ALK*	25-30
	t(2;19)(p23;p13)	*TPM4-ALK*	
	t(2;17)(p23;q23)	*CLTC-ALK*	
	t(2;11) (p23;p15)	*CARS-ALK*	
	inv(2)(p23q35)	*ATIC-ALK*	
	t(2;4)(p23;q27)	*SEC31A-ALK*	
	t(2;12)(p23;p12)	*PPFIBP1-ALK*	10-20
	t(2;5)(p23;q35)	*NPM1-ALK*	
	t(2;2)(p21;p23)	*EML4-ALK*	
	t(2;1)(p21;q21)	*TPM3-ALK*	
	t(2;19)(p21;p13)	*TPM4-ALK*	
	t(2;2)(p23;q13)	*RANBP2-ALK*	
	t(6;3)(q22;q12)	*TFG-ROS1*	6-10
	t(6;17)(q22;p13)	*YWHAE-ROS1*	
	t(5;12)(q32;q13)	*NAB2-PDGFRB*	*
Low grade fibromyxoid sarcoma	t(7;16)(q33;p11)	*FUS-CREB3L2*	60-80
	t(11;16)(p11;p11)	*FUS-CREB3L1*	3-6
	Supernumerary ring	-	25-42
Myoinflammatory fibroblastic sarcoma	t(1;10)(p22;q24)	*TGFBR3-MGEA5*	62-80
	amp(3)(p12)	*VGLL3*	37-50
Infantile fibrosarcoma	t(12 ;15) (p13;q25)	*ETV6-NTRK3*	75-90
Solitary fibrous tumour	inv(12)(q13q13)	*NAB2-STAT6*	44-55
Congenital fibrosarcoma	t(12;15)(p13;q25)	*ETV6-NTRK3*	90-99
Sclerosing epithelioid fibrosarcoma	t(11;22)(p11;q12)	*EWSR1-CREB3L1*	80-90
	t(12;16)(q13;p11)	*DDIT3-FUS*	10-20
	t(7;16)(q33;p11)	*FUS-CREB3L2*	*
	t(11;16)(P13;p11)	*FUS-CREB3L1*	*
So-called Fibrohistiocytic tumours			
Tenosynovial giant cell tumour	t(1;2)(p11;q35-36)	*CSF1-COL6A3*	50-64
Epithelioid fibrous histiocytoma	t(2;10)(q22;p22)	*VCL-ALK*	80-88
	t(2;5)(p23;q35)	*SQSTM1-ALK*	*
Smooth muscle tumours			
Benign metastasizing leiomyoma	del(19)(q13.3), del(22)(q12)	-	#
Uterine leiomyoma	t(12;14)(q14;q22)	*HMGA2-ALDH2*	17-20
Pericytic (perivascular) tumour			
Myopericytoma	t(7;12)(p22;q13)	*ACTB-GLI1*	#
Skeletal muscle tumours			
Embryonal rhabdomyosarcoma	del(11)(p15.5)	*IGF2, H19, CDKN1C, HOTS*	35-45
Alveolar rhabdomyosarcoma	t(2;13)(q35;q14)	*PAX3-FOXO1*	60-85
	t(1;13)(p36;q14)	*PAX7-FOXO1*	15-20
	t(2;2)(q35;p23)	*PAX3-NCOA1*	10-18
	t(2;8)(q35;q13)	*PAX3-NCOA2*	*
	amp(12)(q13-15)	*GLI1, CDK4, MDM2*	22-56
	amp(2)(p24)	*MYCN*	16-50
Vascular tumours			
Epithelioid haemangioma	t(1;3)(p36;q25)	*WWTR1-CAMTA1*	70-90
	t(X;11)(p11;q22)	*YAP1-TFE3*	*
	t(19;19)(q13;q13)	*ZFP36-FOSB*	*
	t(19;1)(q13;q22)	*FOS-LMNA*	*

	t(19;10)(q13;p13)	FOS-VIM	*
Pseudomyogenic haemangioendothelioma	t(7;19)(q22;q13)	SERPINE1-FOSB	20-30
Epithelioid hemangioendothelioma	t(11;X)(q22;p11) t(1;3)(p36;q23)	YAP1-TFE3 WWTR1-CAMTA1	80-94 77-85
Chondro-osseous tumours			
Chondromyxoid fibroma	inv(6)(p25q13) del(6)(q24) t(6;17)(q23;p13) t(6;9)(q25;q22)	- - BCLAF1-RAP1GAP2 COL12A1-?	75-80 20-40 15-20 6-20
Mesenchymal chondrosarcoma	del(8)(q13;q21)/t(8;8)(q21;q13)	HEY1-NCOA2	70-80
Nerve sheath tumour			
Melanotic schwannoma	del(2)(p16)/amp(2)(p16)	CNC2	70-80
Perineurioma	- 22/del(22)(q12) Supernumerary ring	NF2 -	75-80
Schwannoma	- 22q	NF2, SMARCB1	40
Ewing sarcoma			
Ewing sarcoma	t(11;22)(q24;q12) t(21;22)(q22;q12) t(7;22)(p2;q12) t(17;22)(q21;q12) t(2;22)(q35;q12) t(20;22)(q13;q12) inv(22)(q12q12) t(4;22)(q31;q12) t(6;22)(p21;q12) t(2;22)(q31;q12) t(1;22)(p36;q12) t(16;21)(p11;q22) t(2;16)(q35;p11) del(9)(p21) t(4;19)(q35;q13) t(X;X)(p11;p11)	EWSR1-FLI1 EWSR1-ERG EWSR1-ETV1 WESR1-ETV4 EWSR1-FEV EWSR1-NFATC2 EWSR1-ZFG EWSR1-SMARCA5 EWSR1-POU5F1 EWSR1-SP3 EWSR1-PATZ FUS-ERG FUS-FEV CDKN2A CIC-DUX4 BCOR-CCNB3	80-90 12-15 5-10 * * * * * * * * * * * * *
Tumours of uncertain differentiation			
Angiomatoid fibrous histiocytoma	t(2;22)(q33;q12) t(12;22)(q13;q12) t(12;16)(q13;p11)	EWSR1-CREB1 EWSR1-ATF1 FUS-ATF1	75-85 10-14 *
Extraskeletal myxoid chondrosarcoma	t(9;22)(q22;q12) t(9;17)q22;q11) t(9;15)(q22;q21) t(9;22)(q22;q11) t(9;17)(q22;q11) t(9;15)(q22;q21) t(9;22)(q22;q15) t(12;22)(q13;q21)	EWSR1-NR4A3 TAF2N-NR4A3 TFC12-NR4A3 EWSR1-NR4A3 TAF15-NR4A3 TCFI2-NR4A3 TFG-NR4A3 EWSR1-CHOP	50-75 15-20 * * * * * *
Hemosiderotic fibrolipomatous tumour	t(1;10)(p22;q24)	TGFBR3-MGEA5	70-85
Extraskeletal myxoid chondrosarcoma	t(9;22)(q22;q12) t(9;17)q22;q11) t(9;15)(q22;q21) t(9;17)(q22;q11)	EWSR1-NR4A3 TAF2N-NR4A3 TFC12-NR4A3 TAF15-NR4A3	50-75 15-20 * *

	t(9;22)(q22;q15)	*TFG-NR4A3*	*
	t(12;22)(q13;q21)	*EWSR1-CHOP*	*
Alveolar soft part sarcoma	t(X;17)(p11;q25)	*ASPSCR1-TFE3*	80-95
Myoepithelioma/myoepithelial carcinoma/mixed tumour	t(6;22)(p21;q12)	*EWSR1-POU5F1*	23
	t(1;22)(q23;q12)	*EWSR1-PBX1*	16
	t(1;16)(p34;p11)	*FUS-KLF17*	9
	t(9;22)(q33;q21)	*EWSR1-PBX3*	8
	t(19;22)(q13;q12)	*EWSR1-ZNF444*	*
	t(12;22)(q13;q12)	*EWSR1-ATF1*	*
Soft tissue angiofibroma	t(5;8)(p15;q13)	*AHRR-NCOA2*	30-50
Ossifying fibromyxoid tumour	t(6;12)(p21;q24)	*EP400-PHF1*	50-80
	t(1;6)(p34;p21)	*MEAF6-PHF1*	
	t(6;10)(p21;p11)	*EPC1-PHF1*	
	t(X;22)(p11;q13)	*ZC3H7B-BCOR*	*
Clear cell sarcoma of soft tissue	t(12;22)(q13;q12)	*EWSR1-ATF1*	50-75
	t(2;22)(p13;q12)	*EWSR1-CREB1*	6-13
	t(12;16)(q13;p11)	*FUS-ATF1*	*
Clear cell sarcoma of the kidney	t(10;17)(q22;p13)	*YWHAE-NUTM2E*	13-25
Clear cell sarcoma like tumour of GI tract	t(12;22)(q13;q12)	*EWSR1-ATF1*	85-90
	t(2:22)(q33:q12)	*EWSR1-CREB1*	6-20
Desmoplastic small round cell tumour	t(11;22)(p13;q12)	*EWSR1-WT1*	90-99
	t(21;22)(q22;q12)	*EWSR1-ERG*	*
Extraskeletal Ewing sarcoma	t(11;22)(q24;q12)	*EWSR1-FLI1*	80-90
	t(17;22)(q12;q12)	*EWSR1-EIAF*	5-10
	t(21;22)(q22;q12)	*EWSR1-ERG*	*
	t(7;22)(q22;q12)	*EWSR1-ETV1*	*
	t(2;22)(q36;q12)	*EWSR1-FEV*	*
	t(16;21)(p11;q22)	*FUS-ERG*	*
	t(2;16)(q36;p11)	*FUS-FEV*	*
Intimal sarcoma	amp(12)(q13-14)	*CDK4, TSPAN31, MDM2, GLI*	75-100
Primary pulmonary myxoid sarcoma	t(2;22)(q33;q12)	*EWSR1-CREB1*	70-90
PEComa	t(X;17)(p11;p13)	*DVL2-TFE3*	90-100
	t(X; 1)(p11;p34)	*SFPQ-TFE3*	
	inv(X)(p11.2q12)	*NONO-TFE3*	
	t(5;8)(q32;q24)	*HTR4-ST3GAL1*	*
	t(3;3)(p21;p13)	*RASSF1-PDZRN3*	*
	t(x;14)(q12;q24.1)	*RAD51B-RRAGB*	*
Synovial Sarcoma	t(X;18)(p11;q11)	*SYT-SSX1*	65-80
	t(X;18)(p11;q11)	*SYT-SSX2*	31-35
	t(X;18)(p11;q13)	*SYT-SSX4*	*
	t(X;20)(p11;q13)	*SS18L1-SSX1*	*
Undifferentiated/unclassified sarcoma			
Undifferentiated round and spindle cell sarcomas	t(4;19)(q35;q13.1)	*CIC-DUX4*	28-30
	inv(X)(p11.2p11.4)	*BCOR-CCNB3*	3-12

Round cell Ewing-like sarcoma	t(4;19)(q35;q13)	*CIC-DUX4*	60-75
	t(20;22)(q13;q12)	*EWSR1-NFATc2*	*
	t(6;22)(p21;q12)	*EWSR1-POU5F1*	*
	t(4;22)(q31;q12)	*EWSR1-SMARCA5*	*
	inv(22)(q12q12)	*EWSR1-PATZ1*	*
	t(4;22)(q31;q12)	*EWSR1-SMARCA5*	*
	t(1;22)(p36;q12)	*EWSR1- ZSG*	*
	t(2;22)(q31;q12)	*EWSR1-SP3*	*
	t(10;19)(q26;q13)	*CIC-DUX10*	*
	t(X;19)(q13;q13)	*CIC-FOXO4*	*
	t(16;21)(p11;q22)	*FUS-ERG*	*
	t(20;16)(q13;p11)	*FUS-NCATc2*	*
	inv(X)(p11.4p11.22)	*BCOR-CCNB3*	*
	t(12;15)(p13;q25)	*ETV6-NTRK3*	*
Tumour of undefined neoplastic nature			
Aneurysmal bone cyst	t(16;17)(q22;p13)	*CDH11-USP6*	66-72

Data Sources: http://cancer.sanger.ac.uk/cosmic; https://www.mycancergenome.org; http://www.genenames.org; http://atlasgeneticsoncology.org; http://cgap.nci.nih.gov/chromosomes; http://www.genecards.org; www.tumorfusions.org.

*Too infrequent to estimate percentage, # limited reports

Table 2 Chromosome alterations in solid tumours of epithelial origin.

Tumour Type	Chromosome alteration	Gene Involved	%
Head and Neck/Salivary gland			
Pleomorphic adenoma	t(3;8)(p21;q12)	*CTNNB1-PLAG1*	
	t(5:8)(p13;q12)	*LFIR-PLAG1*	
	r(8)(p12q12)	*FGFR1-PLAG1*	
	t(8;8)(q12;q12)	*CHCHD7-PLAG1*	30–40
	t(8;8)(q11;q12)	*TCEA1-PLAG1*	
	t(7;8)(q21;q12)	*COL1A2-PLAG1*	
	t(8;8)(q24;q12)	*HAS2-PLAG1*	
	t(9;12)(p22;q14)	*HMGA2-NFIB*	5-8
	t(3;12)(p14;q14)	*HMGA2-FHIT*	
Adenoid cystic carcinoma	t(6;9)(q22;p23)	*MYB-NFIB*	30–50
Clear cell odontogenic carcinomas	t(22;12)(q12;q13)	*EWSR1-ATF1*	63–82
Hyalinizing clear cell carcinoma	t(22;12)(q12;q13)	*EWSR1-ATF1*	60–85
Mucoepidermoid carcinoma	t(11;19)(q21;p13)	*CRTC1-MAML2*	50–70
	t(15;11)(q26;q21)	*CRTC3-MAML2*	2–6
	t(1;11)(q21;q21)	*CRTC2-MAML2*	*
	t(6;22)(p21;q12)	*EWSR1-POU5F1*	*
Mammary analogue secretory carcinoma	t(12;15)(p13;q25)	*ETV6-NTRK3*	85–94
NUT midline carcinoma	t(15;19)(q13;p13)	*BRD4–NUTM1*	70–80
	t(15;9)(q13;q34)	*BRD3-NUTM1*	10–15
Salivary duct carcinoma	del(10)(q23)	*PTEN*	40–50
	t(12;8)(q14;q12)	*HMGA2-PLAG1*	22-50
Solitary dermal cylindroma	t(6;12)(q23;q23)	*MYB–NFIB*	60–80
Squamous cell carcinoma of the head and neck	Amp(8)(p11)	*FGFR1*	9–15
Thyroid gland			
Papillary thyroid carcinoma	inv(10)(q11q21)	*RET-CCDC6(PTC1)*	60-70
	inv(10)(q11q10)	*RET-NCOA4(PTC3)*	22-30[a]
	t(1;15)(q21;q25)	*NTRK1-TPM3*	12
	t(10;17)(q11;q23)	*RET-PRKAR1A(PTC2)*	5-11[a]
	t(12;15)(p13;q25)	*ETV6-NTRK3[a]*	2-14[a]
	t(10;14)(q11;q32)	*RET- GOLGA5*	*
	t(7;10)(q32;q11)	*RET-TRIM24*	*
	t(10;14)(q11;q32)	*RET-TRIM27*	*
	t(1;10)(p13;q11)	*RET-TRIM33*	*
	t(10;14)(q11;q22)	*RET-KTN1*	*
	t(8;10)(p21;q11)	*RET-PCM1*	*
	t(6;10)(p21;q11)	*RET-TRIM27*	*
	t(8;10)(p11;q11)	*RET-HOOK3*	*
	t(10;12)(q11;p13)	*RET-ERC1*	*
	t(10;18)(q11;q21)	*RET-MBD1*	*
	t(2;2)(p22;p23)	*STRN-ALK*	*
	t(7;7)(q21;q34)	*AKAP9-BRAF*	*
Follicular thyroid carcinoma	t(2;3)(q13;p25)	*PAX8-PPARγ*	30-35

Medullary thyroid carcinoma	t(10;17)(q11;p13)	*RET-MYH13*	#
Lung			
Lung adenocarcinoma	inv(2)(p21p23)	*EML4-ALK*	3-7
	t(2;3)(p23;q12)	*TFG-ALK*	
	t(2;10)(p23;p11)	*KIF5B-ALK*	
	t(2;14)(p23;q32)	*KLC1-ALK*	
	t(2;9)(p23;q31)	*PTPN3-ALK*	1-2
	t(2;2)(p23;p22)	*STRN-ALK*	
	t(2;4)(p23;q21)	*SEC31A-ALK*	
	t(2;7)(p23;q11)	*HIP1-ALK*	
	t(6;10)(q22;q21)	*CCDC6-ROS1*	
	t(6;7)(q22;p22)	*KDELR2-ROS1*	
	t(6;12)(q22;q14)	*LRIG3-ROS1*	
	t(6;20)(q22;q13)	*SDC5-ROS1*	
	t(6;5)(q22;q32)	*CD74-ROS1*	2-3
	t(6;19)(q22;q13)	*FIG-ROS1*	
	t(6;6)(q22;q25)	*EZR-ROS1*	
	t(6;1)(q22;q21)	*TPM3-ROS1*	
	t(4;6)(p15;q22)	*SLC34A2-ROS1*	
	t(1;17)(q23;p11)	*MPRIP-NTRK1*	
	t(1;5)(q23;q33)	*CD74-NTRK1*	1-3
	inv(1)(q23q21)	*TPM3-NTRK1*	
	t(10;10)(q11;p11)	*KIF5B-RET*	
	t(10;10)(q11;q21)	*CCDC6-RET*	
	t(10;10)(q11;q11)	*NCOA4-RET*	1
	t(1;10)(p13;q11)	*TRIM33-RET*	
	t(9;7)(q21;q33)	*TRIM24-NTRK2*	#
Primary pulmonary myxoid sarcoma	t(2;22)(q33;q12)	*EWSR1-CREB1*	70-90
Pleura and peritoneum			
Mesothelioma	t(14;22)(q23;q12)	*EWSR1-YY1*	*
Gastrointestinal tract			
Colorectal carcinoma	t(6;6)(q22;q22)	*PTPRK-RSPO3*	5-8
	t(11;2)(p15;p11)	*EIF3E-RSPO2*	3-4
	t(2;2)(p23;p23)	*WDCP-ALK*	
	inv(2)(p21p23)	*EML4-ALK*	2-5
	t(4;6)(p15;q22)	*SLC34A2-ROS1*	0.4-0.8
	t(10;10)(q25;q25)	*NAV2-TCF7L1*	*
	t(8;8)(q23;q23)	*VTI1A-TCF7L2*	*
	t(1;1)(q21;q23)	*NTRK1-TPM3*	*
Esophageal adenocarcinoma	t(3;8)(p14.2;q24)	*FHIT-RNF139*	#
Fibrolamellar hepatocellular carcinoma	t(19;19)(p13.1;p13.2)	*DNAJB1-PRKACA*	92–100
Intrahepatic cholangiocarcinoma	t(1;1)(q23;q25)	*RABGAP1L-NTRK1*	*
Gynaecological tract			
Endometrial stromal sarcoma	t(7;17)(p15;q11)	*JAZF1-SUZ12*	40-50
	t(7;10)(p13;q23)	*YWHAE-NUTM2A*	20-30
	t(7;10)(p13;q23)	*YWHAE -NUTM2B*	
	t(1;6)(p34;p21)	*MEAF6-PHF1*	
	t(6;7)(p21;p15)	*JAZF1-PHF1*	6–10

	t(6;10)(p21;p11)	*EPC1-PHF1*	
Ovarian papillary cystadenocarcinoma	t(6;14)(q21;q24)	-	32-40
Breast			
Secretory breast carcinoma	t(12;15)(p13;q25)	*ETV6-NTRK3*	56–100
	t(8;11)(p12;q14)	*TENM4-NRG1*	*
	t(3;6)(q26;q25)	*TBL1XR1-RGS17*	*
	dic(8;11)(p12;q14)	*TENM4-NRG1*	*
Triple-negative breast carcinoma	t(1;1)(p13;q44)	*MAGI3–AKT3*	1
The urinary system and male genital organs			
Oncocytoma	t(5;11)(q35;q13)	-	#
	t(6;9)(p12;p24)	-	#
Metanephric adenoma	t(1;22)(q22;q13)	*EWSR1-PBX1*	*
	t(15;16)(q21;p13)	-	*
	t(9;15)(p24;q24)	-	#
	inv(12)(q13q15)	-	#
	t(1;22)(q22;q13)	-	#
	t(15;16)(q21;p13)	-	#
Clear cell renal cell carcinoma	del(3)(p11-pter)	*VHL, PBRM1, BAP1, SETD2*	70–90
	del(14)(q23)	*HIF1A*	35–40
Papillary renal cell carcinoma	+ 7	*MET*	80
	+ 17	-	85
	-Y	-	70
Renal carcinomas associated with Xp11.2 translocations	t(X;1)(p11.2;q21)	*PRCC–TFE3*	60-70
	t(X;1)(p11.2;p34)	*SFPQ–TFE3*	10-20
	t(X;17)(p11.2;q25)	*ASPSCR1–TFE3*	5-7
	inv(X)(p11.2q12)	*NONO–TFE3*	*
	t(X;17)(p11.2;q23)	*CLTC–TFE3*	*
	t(X;17)(p11.2;q21.3)	*LUC7L3-TFE3*	*
	t(X;19)(p11.2;p13.3)	*KHSRP-TFE3*	*
Renal cell carcinoma associated with t(6;11) translocations	t(6;11)(p21;q12)	*MALAT1-TFEB*	90–100
	t(6;6)(p21;q11)	*KHDRBS2-TFEB*	#
Chromophobe renal cell carcinoma	- 1	-	
	- 2	-	
	- 6	-	
	-10	-	70–90
	- 13	-	
	- 17	-	
	- 21	-	
Renal medullary carcinoma	t(1;22)(q41;q11)	*SMARCB1-CAPN2*	#
	t(15;22)(q22;q11)	*SMARCB1-RORA*	#
	t(11;22)(q21;q11)	*SMARCB1-MAML2*	#
	t(11;22)(q13;q11)	*SMARCB1-MALAT1*	#
ALK translocation associate renal cell carcinoma [b]	t(2;1)(p23;q21)	*TPM3-ALK*	100
	t(2;10)(p23;q22)	*VCL-ALK*	#
Wilms tumour	i(17)(q10)	-	*
	i(7)(q10)	-	#
Clear cell sarcoma of the kidney	t(10;17)(q22;p13)	*YWHAE-NUTM2E*	13-25
Urothelial carcinoma	Polysomy 3	-	
	Polysomy 7	-	80–94[c]
	Polysomy 17	-	
	del(9)(p21)	*CDKN2A*	

	t(4;7)(p16;q22)	*FGFR3-BAIAP2L1*	5-9
	t(4;4)(p16;p16)	*FGFR3-TACC3*	3-6
	t(12;16)(q13;p13)	*SCN8A-GRIN2A*	#
Prostatic adenocarcinoma	t(21;21)(q22;q22)	*TMPRSS2-ERG*	
	t(21;16)(q22;q13)	*HERPUD1-ERG*	47–79
	t(21;1)(q22;q32)	*SLC45A3-ERG*	
	t(21;8)(q22;q24)	*NDRG1-ERG*	
	t(7;22)(p21;q22)	*ETV1-ERG*	*
	t(17;22)(q21;q22)	*ETV4-ERG*	*
	t(7;21)(p21;q22)	*TMPRSS2-ETV1*	
	t(7;1)(p21;q32)	*SLC45A3-ETV1*	
	t(7;15)(p21;q21)	*C15orf21-ETV1*	
	t(7;7)(p21;q15)	*HNRPA2B1-ETV1*	7–10
	t(7;11)(p21;p15)	*ASCL3-ETV1*	
	t(7;14)(p21;q13)	*EST14-ETV1*	
	t(7;17)(p21;p13)	*HERVK17-ETV1*	
	t(1;1)(q32;q32)	*TMPRSS2-ETV4*	*
	t(17;21)(q21;q22)	*CANT1-ETV4*	*
	t(17;17)(q21;q25)	*KLK2-ETV4*	*
	t(3;21)(q27;q22)	*TMPRSS2-ETV5*	*
	t(3;1)(q27;q32)	*SLC45A3-ETV5*	*
	t(17;19)(q21;q13)	*SLC45A3-ELK4*	*
	t(3;8)(p25;q22)	*ESRP1-RAF1*	*
	t(7;1)(q34;q32)	*SLC45A3-BRAF*	*
	del(10)(q23)	*PTEN*	40-70
Testicular germ cell tumour	i(12p)	-	67–83
Skin			
Spitz nevi	t(5;6)(q33;q22)	*PWWP2A-ROS1*	
	t(6;6)(p22;q22)	*HLA-A-ROS1*	
	t(6;12)(q22;p11)	*PPFIBP1-ROS1*	
	t(6;15)(q22;q21)	*MYO5A-ROS1*	
	t(6;12)(q22;p13)	*ERC1-ROS1*	15–20
	t(6;12)(q22;q24)	*CLIP1-ROS1*	
	t(6;12)(q22;q24)	*ZCCHC8-ROS1*	
	t(6;10)(q22;q25)	*SHTN1-ROS1*	
	t(3;6)(q12;q22)	*TFG-ROS1*	
	t(2;2)(p23;p23)	*DCTN1-ALK*	11–15
	t(1;2)(q23;p23)	*TPM3-ALK*	
	t(1;17)(q23;p13)	*TP53-NTRK1*	7–16
	t(1;1)(q23;q22)	*LMNA-NTRK1*	
	t(10;14)(q11;q32)	*GOLGA5-RET*	3
	t(10;10)(q11;p11)	*KIF5B-RET*	
	t(7;19)(q34;q13)	*CEP89-BRAF*	*
	t(7;19)(q34;q13)	*LSM14A-BRAF*	*
	t(2;7)(q37;q31)	*LRRFIP1-MET*	*

Melanoma	amp(11)(q13)	*CCND1*	54–82[d]
	amp(6)(p25)	*RREB1*	
	amp(6)(q23)	*MYB*	
	t(1;7)(q32;q34)	*SLC45A3-BRAF*	*
	t(4;7)(q25;q34)	*PAPSS1-BRAF*	*
	t(7;7)(q33;q34)	*TRIM24-BRAF*	*
	t(7;7)(q34;q34)	*AGK-BRAF*	*
	t(7;7)(p22;q34)	*MAD1L1-BRAF*	*
	t(7;7)(q11;q34)	*KCTD7-BRAF*	*
	t(7;7)(p13;q34)	*NUDCD3-BRAF*	*
	t(7;11)(q34;p15)	*SOX6-BRAF*	*
	t(7;7)(q22;q34)	*ZKSCAN5-BRAF*	*
	t(7;19)(q34;p13)	*PLIN3-BRAF*	*
	t(7;7)(q22;q31)	*ZKSCAN1-MET*	*
	t(7;7)(q22;q31)	*TRIM4-MET*	*
	t(3;8)(p25;q22)	*ESRP1-RAF1*	*
Nervous system			
Oligodendrogliomas	del(1)(p36), del(19)(q13)	-	77-92
	t(1;19)(q10;p10)	-	#
Glioblastomas	del(10)(q23)	*PTEN*	43
	t(7;7)(q31;q31)	*PTPRZ1-MET*	15-35
	t(4;4)(p16;p16)	*FGFR3-TACC3*	5-8
	t(4;8)(p16;p11)	*FGFR1-TACC3*	
	t(3;?)(p27;?)	*?-BCL6*	5
	t(7;7)(p11;p12)	*LANCL2- SEPT14*	*
Angiocentric glioma	t(6;6)(q23;q26)	*MYB-QKI*	80
Pilocytic astrocytoma	t(7;7)(q34;q34)	*KIAA1549-BRAF*	64–73
	t(7;5)(q34;q35)	*RNF130-BRAF*	*
	t(9;6)(q21;q26)	*QKI-NTRK2*	*
Medulloblastoma	i(17q)	-	30–50
	t(1;19)(q23;p13)	*E2A-PBX1*	#
Meningioma	del(22)(q12)	*NF2*	50-60
	t(12;22)(p13;q12)	*MN1-ETV6*	#
	t(1;19)(q21;q13.3)	-	#
Ependymoma	-del(22)(q11)	-	20–30
	t(11;11)(q13;q13)	*C11orf95-RELA*	71–80
	t(2;14)(p23;q22)	*KTN1-ALK*	#
	del(2)(p16p23)	*CCDC88A-ALK*	#
Extraventricular neurocytoma	t(1;19)(q10;p10)	-	17-20
Papillary glioneuronal tumour	t(9;17)(q31;q24)	*SLC44A1-PRKCA*	#

Data Sources: http://cancer.sanger.ac.uk/cosmic; https://www.mycancergenome.org; http://www.genenames.org; http://atlasgeneticsoncology.org; http://cgap.nci.nih.gov/chromosomes; http://www.genecards.org; www.tumorfusions.org.

* Too infrequent to estimate percentage, # limited report

a: Higher incidence in radiation induced thyroid cancers

b: 50% with sickle-cell trait

c: The UroVysion Bladder Cancer Kit (UroVysion Kit) is FDA approved and designed to detect aneuploidy for chromosomes 3, 7, 17, and loss of the 9p21 locus in urothelial tumours.

d: The Vysis Melanoma FISH Probe Kit is designed to detect copy number of the RREB1 (6p25), MYB (6q23), CCND1 (11q13) genes and of centromere 6 in melanocytic lesions.
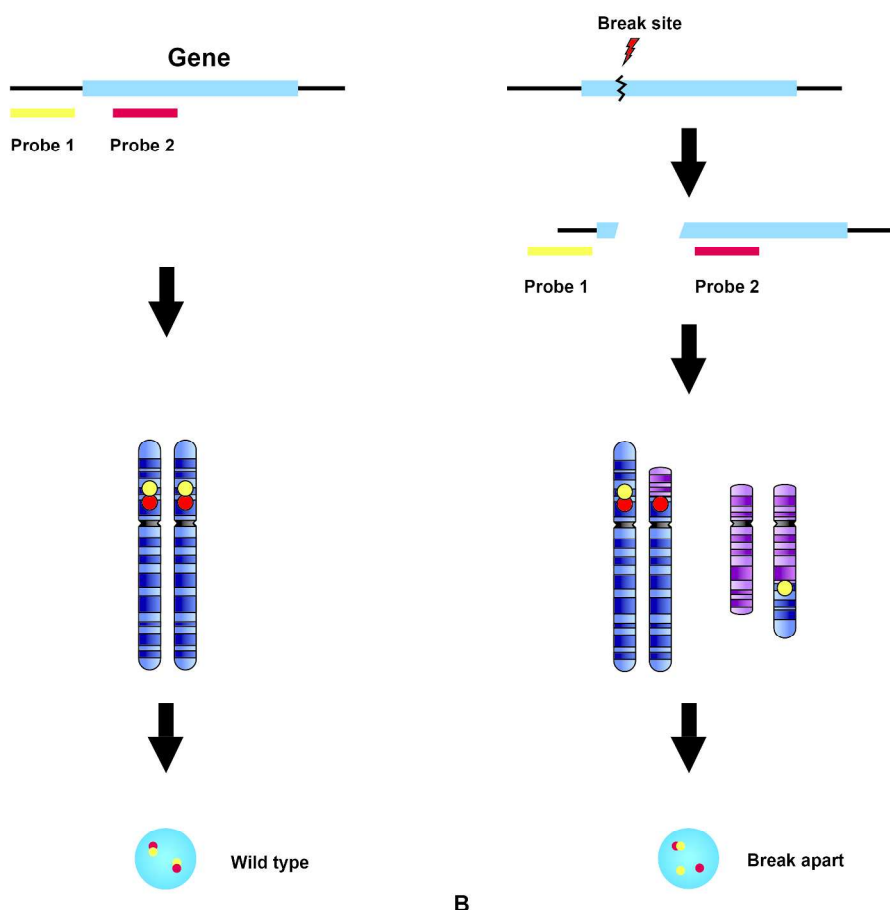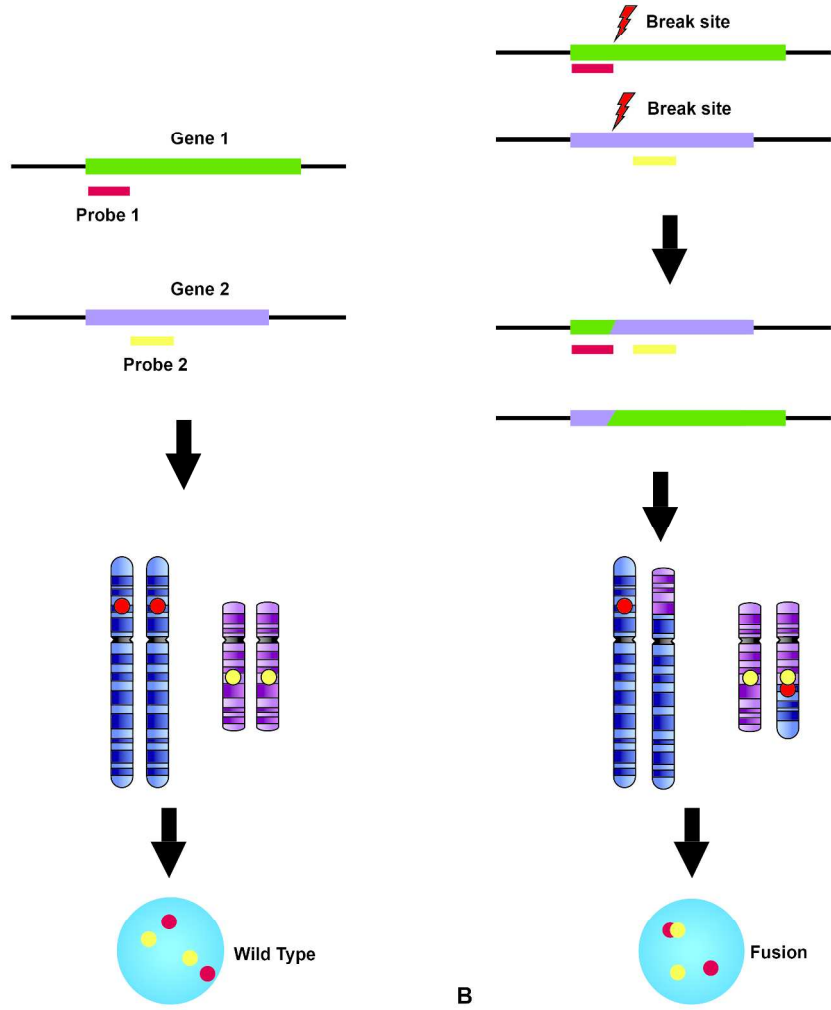
Figure 1

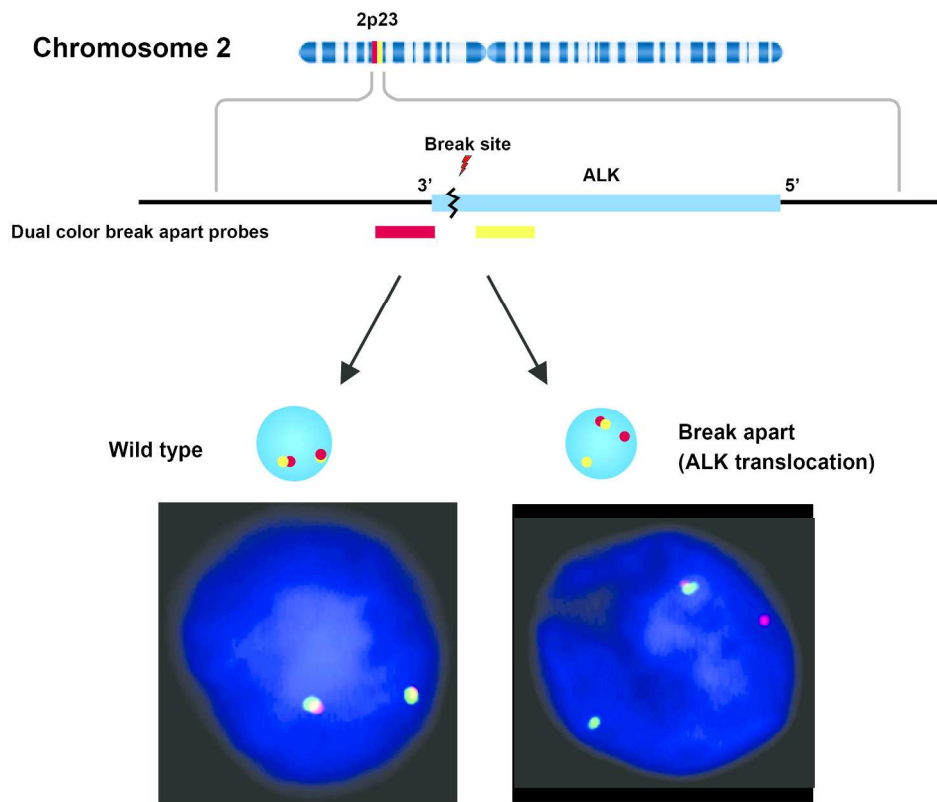279x270mm (300 x 300 DPI)

Figure 2

279x301mm (300 x 300 DPI)

Figure 3

232x199mm (300 x 300 DPI)

A

B

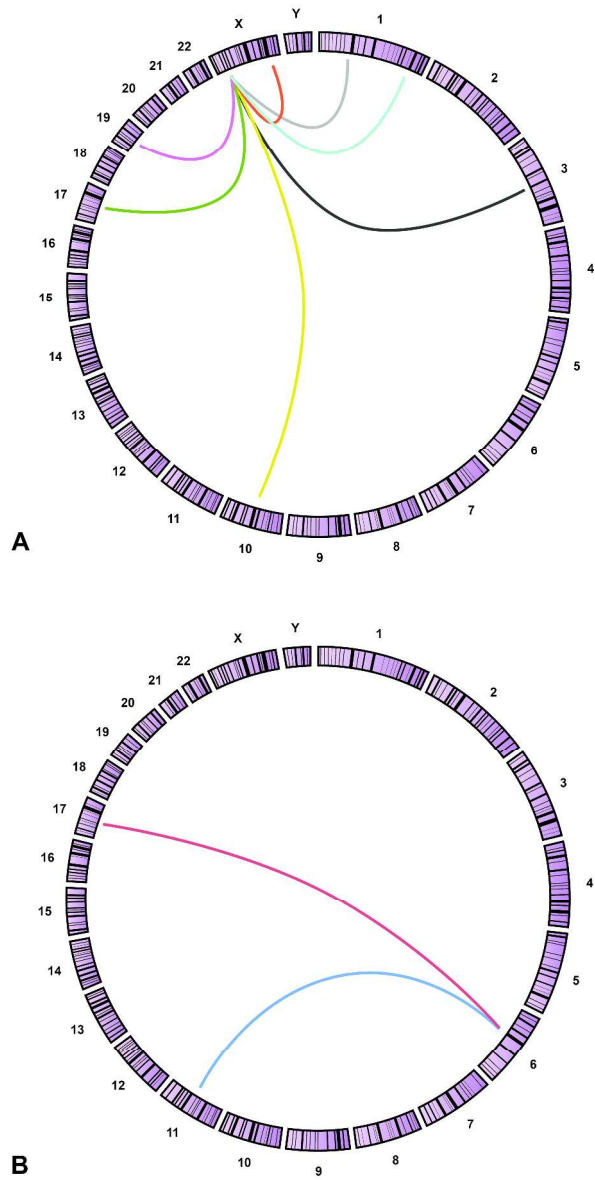Figure 4

324x608mm (300 x 300 DPI)
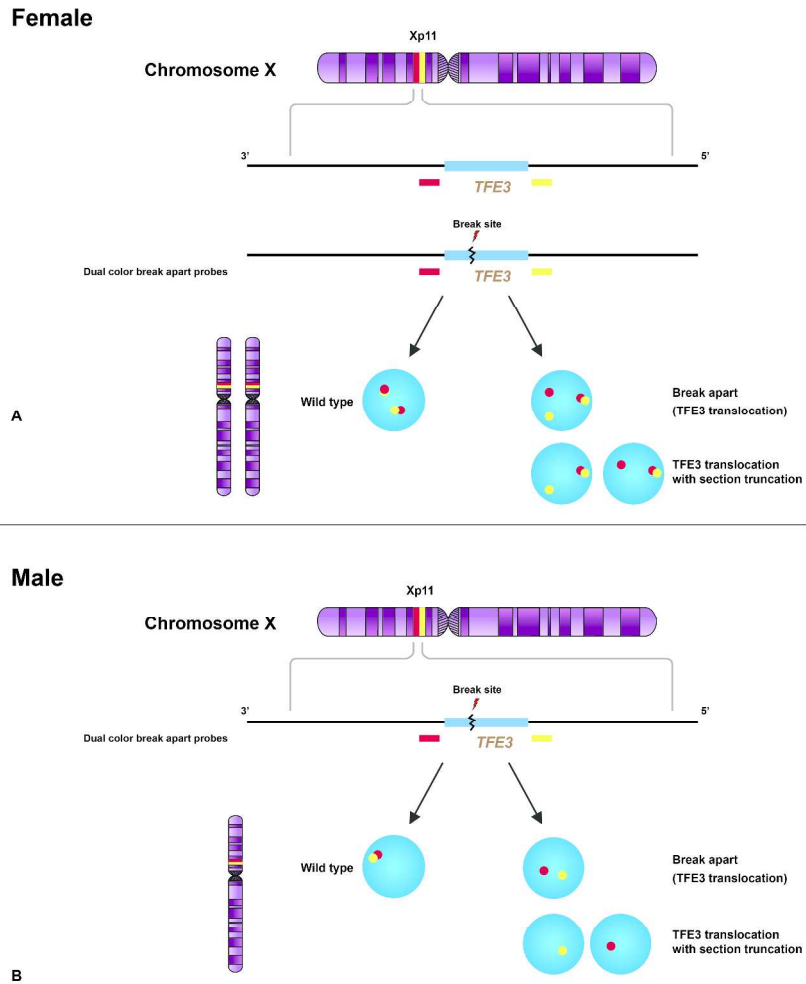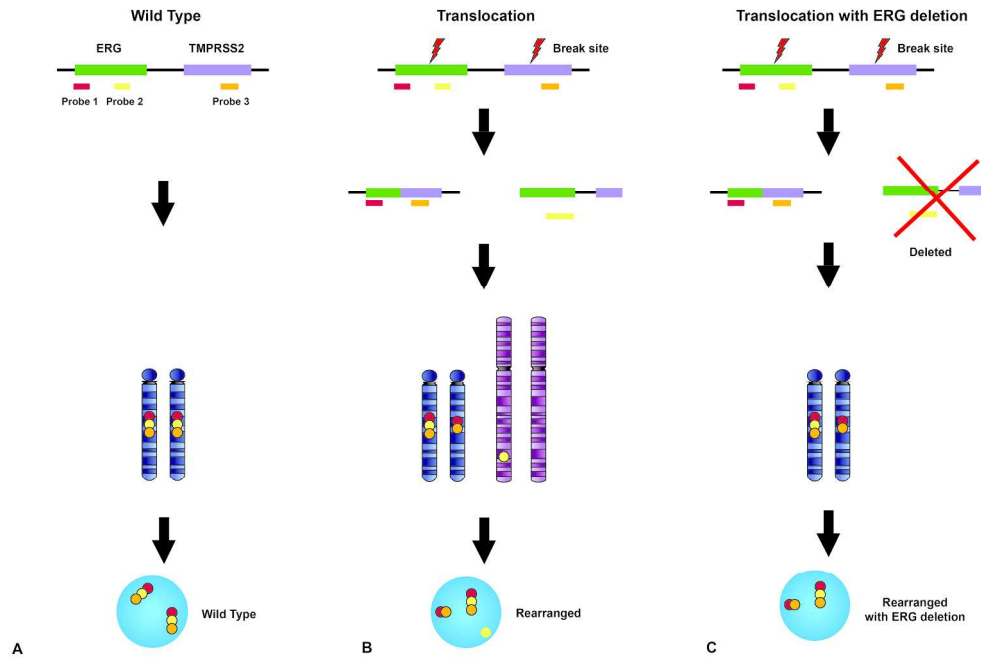
Figure 5

415x429mm (300 x 300 DPI)

Figure 6

235x157mm (300 x 300 DPI)